Contents lists available at ScienceDirect

Neurobiology of Stress

Restoring tripartite glutamatergic synapses: A potential therapy for mood and cognitive deficits in Gulf War illness

Xueqin Wang [a], Zan Xu [a], Fangli Zhao [a], Kuanhung J. Lin [a], Joshua B. Foster [a], Tianqi Xiao [a], Nydia Kung [a], Candice C. Askwith [a], John P. Bruno [a,b], Valentina Valentini [b,c], Kevin J. Hodgetts [d], Chien-liang Glenn Lin [a,*]

[a] Department of Neuroscience, College of Medicine, The Ohio State University, Columbus, OH, USA
[b] Department of Psychology, College of Arts and Sciences, The Ohio State University, Columbus, OH, USA
[c] Department of Biomedical Sciences, University of Cagliari, Italy
[d] Department of Neurology, Brigham and Women's Hospital, Harvard Medical School, Cambridge, MA, USA

ARTICLE INFO

ABSTRACT

Gulf War illness is associated with a combination of exposure to war-related chemical agents and traumatic stress. Currently, there are no effective treatments, and the pathophysiology remains elusive. Neurological problems are among the most commonly reported symptoms. In this study, we investigated the glutamatergic system in the hippocampi of mice exposed to war-related chemical agents and stress. Mice developed Gulf War illness-like symptoms, including mood deficits, cognitive impairments, and fatigue. They exhibited the following pathological changes in hippocampi: elevated extracellular glutamate levels, impaired glutamatergic synapses, astrocyte atrophy, loss of interneurons, and decreased neurogenesis. LDN/OSU-215111 is a small-molecule that can strengthen the structure and function of both the astrocytic processes and the glutamatergic synapses that together form the tripartite synapses. We found that LDN/OSU-215111 effectively prevented the development of mood and cognitive deficits in mice when treatment was implemented immediately following the exposure. Moreover, when symptoms were already present, LDN/OSU-215111 still significantly ameliorated these deficits; impressively, benefits were sustained one month after treatment cessation, indicating disease modification. LDN/OSU-215111 effectively normalized hippocampal pathological changes. Overall, this study provides strong evidence that restoration of tripartite glutamatergic synapses by LDN/OSU-215111 is a potential therapy for Gulf War illness.

1. Introduction

Gulf War illness (GWI) is a chronic and multi-symptomatic disorder affecting approximately one third (~175,000 to 210,000) of Gulf War (GW) veterans (Nettleman, 2015). The symptoms vary among individuals and include cognitive difficulties, mood problems, chronic headache, sleep problems, debilitating fatigue, widespread pain, respiratory symptoms, gastrointestinal problems, and dermatological complaints (Cory-Slechta and Wedge, 2016). Nervous system problems are frequently reported (Gray et al., 2002; Kang et al., 2009; Toomey et al., 2009; White et al., 2016). It is widely believed that these clinical symptoms are linked to a combination of war-related traumatic stress and exposure to chemical agents, such as pyridostigmine bromide (given to soldiers as an anti-nerve agent pretreatment), sarin nerve agent, pesticides, and smoke from burning oil wells (Fulco et al., 2000; Haley and Kurt, 1997; Steele et al., 2012; Wolfe et al., 2002). The long-term

effects of such combined exposures in rodents have been extensively studied and indicate that exposed rodents developed GWI-like symptoms, such as increased anxiety- and depression-like behaviors and cognitive impairments (Carreras et al., 2018; Hattiangady et al., 2014; Kodali et al., 2018; Parihar et al., 2013; Zakirova et al., 2015). However, the underlying mechanisms linking the exposure, the pathological changes, and the symptoms have not been elucidated.

Pyridostigmine bromide, pesticides, and sarin are organophosphate or carbamate acetylcholinesterase inhibitors (Colovic et al., 2013; Golomb, 2008). Under stress conditions, they can enter the brain and inhibit acetylcholinesterase activity leading to increased acetylcholine levels, which result in enhanced spontaneous glutamate release via overactivation of muscarinic receptors located on presynaptic terminals (Meyer and Shafer, 2006; Pavlovsky et al., 2003). Moreover, mounting evidence indicates that stress can cause dysregulation of glutamate transmission (Musazzi et al., 2010; Raudensky and Yamamoto, 2007; Yuen et al., 2009). Thus, chronic exposure to GW-related agents and stress could result in increased extracellular glutamate levels (Macht et al., 2020), which could cause excitotoxic damage and synaptic dysfunction (Li et al., 2011). It has been reported that exposure to an organophosphate pesticide, individually or in combination with other GW agents, results in the impairment of hippocampal synaptic integrity in mice (Abdel-Rahman et al., 2001; Ojo et al., 2014). In addition, it has been shown that stress causes loss of dendrites and their synapses, leading to decreased grey matter volume in the hippocampus (Kassem et al., 2013). Abdel-Rahman *et al.* reported that exposure to a combination of stress and GW agents significantly decreases the thickness of hippocampal CA3 and CA1 in rats (Abdel-Rahman et al., 2004). Importantly, reduced hippocampal volume and hippocampal dysfunction have been extensively reported in veterans with GWI (Apfel et al., 2011; Chao et al., 2017; Vythilingam et al., 2005). Taken together, current literature indicates that traumatic stress and GW agents can cause hippocampal abnormalities and atrophy, which may result in or contribute to many neurological problems in veterans with GWI. In the present study, we investigated the underlying mechanisms of hippocampal abnormalities in a mouse model of GWI.

Furthermore, we investigated whether restoration of hippocampal deficits could serve as a potential therapeutic strategy. We have discovered and developed a novel series of small-molecules, pyridazine derivatives, which can strengthen the structure and function of both the astrocytic processes and the glutamatergic synapses that together form the tripartite synapses (Foster et al., 2018, 2019; Kong et al., 2014; Takahashi et al., 2015). Studies on the mechanism of action reveal that pyridazine derivatives activate local translation of a subset of transcripts in the peri-synaptic astrocytic processes (PAP) (Foster et al., 2018). This results in rapidly up-regulating a subset of astrocytic proteins and enhancing the plasticity of the PAP. Importantly, enhanced plasticity of PAP subsequently leads to increased synaptic protein expression in the synapse and strengthened synaptic long-term potentiation (LTP) (Foster et al., 2018). We have demonstrated that pyridazine derivatives are capable of normalizing glutamate dyshomeostasis and restoring synapse integrity; they exhibit profound efficacy in several disease models, including Alzheimer's disease, amyotrophic lateral sclerosis, and epilepsy (Foster et al., 2019; Kong et al., 2014; Takahashi et al., 2015). In the present study, we investigated an advanced small-molecule, LDN/OSU-215111, in GWI mice and found that LDN/OSU-215111 effectively normalized hippocampal deficits and ameliorated symptoms.

2. Materials and methods

2.1. Primary antibodies and reagents

The following primary antibodies were used: actin (Sigma-aldrich, MAB1501), doublecortin (Abcam, ab18723), EAAT2 (custom antibody) (Kong et al., 2014), GABA$_A$ R α 1 (GeneTex, GTX133261), GAPDH (Santa cruz, sc-365062), Gephyrin (GeneTex, GTX109734), GFAP (Sigma-aldrich, G3893), parvalbumin (Sigma-aldrich, P3088), PSD95 (Cell Signaling Technology, 3450S), synaptophysin (Cell Signaling Technology, 9020S), vGAT (Thermo fisher, PA5-96231), and vGLUT1 (Sigma-aldrich, MAB5502).

The following reagents were used: acetonitrile (Fisher scientific, A21-4), adenosine 5′-triphosphate magnesium salt (Mg ATP, Sigma-aldrich, A9187), boric acid (Fisher scientific, A73-500), CaCl$_2$ (Fisher scientific, C79-500), citric acid (Fisher scientific, A104-500), CsCl (Fisher scientific, BP210-500), D-glucose (Fisher scientific, D16-500), EDTA (Fisher scientific, S311-500), EGTA (Acros Organics, 409911000), ethanol (Fisher scientific, BP28184), guanosine 5-triphosphate sodium salt hydrate (Na$_3$GTP, Sigma-aldrich, G8877), HEPES (Fisher scientific, BP310-100), KCl (Fisher scientific, P330-500), KH$_2$PO$_4$ (Fisher scientific, BP362-500), KOH (Fisher scientific, P250-500), kynurenic acid (Sigma-aldrich, K3375), L-glutamic acid hydrochloride (Sigma-aldrich, G2128), methanol (Fisher scientific, A452-1), MgCl$_2$ (Fisher scientific, M33-500), MgSO$_4$ (Fisher scientific, M65-500), NaCl (Fisher scientific, S271-3), NaHCO$_3$ (Fisher scientific, S233-500), NaH$_2$PO$_4$ (Fisher scientific, S397-500), N, N-diethyl-meta-toluamide (DEET, Sigma-aldrich, D100951), ortho-phthalaldehyde (Pickering Laboratories, O120), paraformaldehyde (Acros Organics, 416780010), perchloric acid (Sigma-aldrich, 311421), permethrin (Sigma-aldrich, 45614), phosphoric acid (Fisher scientific, A242-500), pyridostigmine bromide (Sigma-aldrich, P9797), sucrose (Fisher scientific, S5-500), sodium azide (Fisher scientific, S2271-100), sodium sulfite (Fisher scientific, S447-500) and tetrodotoxin (Abcam, ab120054).

2.2. Animals

Wild-type C57BL/6J mice (The Jackson Laboratory, 000664) were used and housed in a room at 24 °C on a 12-h light/dark cycle with free access to food and water *ad libitum*. All procedures were approved by the Institutional Animal Care and Use Committee of The Ohio State University following the National Institutes of Health Guide for the Care and Use of Laboratory Animals.

2.3. A GWI mouse model and LDN/OSU-215111 treatment

Three-month old C57BL/6J mice were exposed to GW agents and traumatic stress daily for six weeks. GW agents included (I) pyridostigmine bromide, which was given by voluntarily oral feeding (1.3 mg/kg, 100 μl in ddH$_2$O), (II) permethrin, which was applied on shaved skin areas located on the back of the neck (0.13 mg/kg, 100 μl in 70% ethanol), and (III) DEET, which was also applied on the skin as permethrin (40 mg/kg) (Parihar et al., 2013). GW agents were administrated in the morning (8–9 am) followed by introduction of unpredictable stress. The stress regimen consisted of exposure to two different stressors each day, including restraint (1 h), cage rotation (25 rpm, 1 h), hot stress (37 °C, 1 h), cold stress (4–8 °C, 1 h), wet bedding (4 h), replace bedding with water (0.5 cm in height, 3 h), and cage tilt at 45° angle (4 h) (Duric et al., 2010).

LDN/OSU-215111 was given at 5–6 pm to avoid the reaction with GW agents. LDN/OSU-215111 has high solubility and easily dissolves in ddH$_2$O. The dissolved LDN/OSU-215111 (100 mg/ml) was mixed with 50% honey (100 μl per mouse) and administrated by voluntary feeding at 10 mg/kg, vehicle-treated mice received 100 μl of 50% honey. Control mice were handled in the same manner as GWI mice with the exception of no exposure to GW agents and stress. Body weight was measured every Tuesday morning before exposure to GW agents and stress.

2.4. Behavioral studies

Examiners were blinded to the treatment groups. Mice were habituated in test room for at least 30 min before the test. Tests were performed during the light phase of the circadian cycle (10 a.m. - 5 p.m.), and illumination was 20 lux, unless specific emphasized. We conducted

one test per-day and started with the least stressful test to reduce any potential effects from previous tests. The order of the tests was open field, light/dark transition, elevated plus maze, novelty suppressed feeding, tail suspension, novel object recognition, Barnes maze, wire-hanging and inverted grid suspension. The video was recorded by a web camera and data analyzed using an automatic video-tracking system (Harvard Apparatus, SMART v3.0), except for novelty suppressed feeding, wire-hanging, and inverted grid suspension tests, which were analyzed manually. Between each mouse, 70% ethanol solution was used to clean the apparatus, when all the mice have been tested, Opti-Cide[3] cleaner (Micro-Scientific, OCP04-128) was used as disinfectant.

2.4.1. Open field

Mice were placed in a corner of grey rectangle box ($30 \times 27 \times 30$ cm) for 10 min. A rectangle zone (15×13.5 cm) in the center of box was defined as center area. The percentage of time spent in the center and total distance traveled were measured.

2.4.2. Light/dark transition

This test was performed as previously reported (Serchov et al., 2016). The apparatus consisted of a rectangle box ($45 \times 14 \times 15$ cm) with one third of dark chamber and two thirds of brightly illuminated chamber; a restricted 3×4 cm opening connects the two chambers. The illumination in the light chamber is 200 lux or more, while the dark chamber is 5 lux or less. Mice were placed in a corner of the light chamber facing away from the door, released and recorded free moving for 5 min, the percentage of time spent in the light chamber was used for analysis.

2.4.3. Elevated plus maze

This test was performed as previously reported with a plus-shaped apparatus (Knowland et al., 2017), the length of arm is 35 cm, the width is 5 cm, with 12 cm height walls flanking on two opposite arms (closed arms), and it is elevated 55 cm from a table. Mice were placed in the center of the apparatus and recorded free moving for 10 min. The percentage of time spent in the open arms was used for analysis.

2.4.4. Novelty suppressed feeding

This test was performed under normal room illumination. The apparatus consisted of a dark grey plastic box ($55 \times 30 \times 17$ cm). Mice were food deprived for overnight (15–16 h) before the test. During the test, a single pre-weighted food pellet was placed at the center of the box, and mice were allowed to move freely in the arena. The test ended when the first bite happened or up to 10 min. Mice were then returned to their home cage with the food pellet for 5 min to determine whether the mice had similar desire to eat. The latency of first bite was used for analysis. If no bite happened during the 10 min period, 10 min were used instead.

2.4.5. Tail suspension

This test was performed under normal room illumination as previously described (Knowland et al., 2017). Briefly, mice were suspended by tails with adhesive tape 1 cm from tip of tail and roughly 40 cm off the ground so no contact could be made. Pre-cut 1000 µl pipette tips were placed over mice tails to prevent climbing or hanging on to their tail. Mice were video recorded for 10 min, and time spent immobile in the last 6 min was analyzed.

2.4.6. Novel object recognition

This test was used to assess non-spatial long-term memory and was performed as previously described (Leger et al., 2013). On day 1 and day 2, mice were allowed free moving in an empty arena ($33 \times 25 \times 25$ cm) for 10 min. On day 3, two identical objects (familiar) were placed equidistant on opposite ends of the arena, and mice were explored in the arena for 10 min. On day 4, one of the objects was replaced by a novel object with similar texture, size, and odor. Time spent with each object was analyzed. Data were presented as discrimination index, discrimination index = $(\text{Time}_{novel} - \text{Time}_{familiar})/(\text{Time}_{novel} + \text{Time}_{familiar})$. Higher number indicated that mice spent more time with novel object.

2.4.7. Barnes maze

This test was used to assess spatial learning memory and was performed as previously described (Sunyer et al., 2007). The paradigm consisted of a grey circular platform (92 cm of diameter) with 20 equally spaced holes (5 cm diameter, 7.5 cm between holes and 2 cm away from the edge) along the perimeter, which was elevated 105 cm above the floor. An escape box was placed underneath a certain hole (target hole); the location of escape box was fixed but the platform could be rotated to avoid any odor cue. Four different colors and shapes (triangle, rectangle, circle and cross) material were placed on the room wall surrounding the maze as visual cues. Bright light (>200 lux) and noise (electronic metronome, 125 bpm) used as stimulus to force mice enter the escape box. The procedure included three phases: habituation (day 1), training (day 2 and 3), and probe (day 5). During the day 1–3, mice were trained to enter the escape box. On day 5, the escape box was removed, and the mice were allowed to explore freely on the maze for 2 min. The latency to reach the target hole and the time spent in the target quadrant were analyzed.

2.4.8. Wire-hanging

A single 35 cm length, with a diameter of 2 mm metal wire was mounted between two stands. A standard mouse cage was filled with cotton padding and placed under it, the distance between the wire and the cotton surface was 30 cm. Mice were gently placed in the middle of wire, and the latency of drop off was recorded. The test was repeated four times, and average from each mouse was used for analysis.

2.4.9. Inverted grid suspension

A food rack (1 mm diameter wires and 1 cm spacing) from the mouse's home cage and a 4-L beaker were used. The beaker was filled with cotton padding. Mice were gently placed on the food rack, the rack was slowly inverted, and then put the rack on the top of beaker to prevent mice from climbing to the top. The distance from the rack to cotton surface is 20 cm. The latency of drop off was recorded. The test was repeated four times, and average from each mouse was used for analysis.

2.5. Electrophysiological studies

Briefly, mice were anaesthetized with isoflurane (Piramal), the brains were quickly removed and placed in ice-cold cutting solution containing 250 mM sucrose, 25 mM D-glucose, 2.5 mM KCl, 24 mM NaHCO$_3$, 1.25 mM NaH$_2$PO$_4$, 2.0 mM CaCl$_2$, 1.5 mM MgSO$_4$, and 1.0 mM kynurenic acid; pH 7.3–7.4. Coronal sections of 400 µm were sliced on a vibratome (Leica, VT1200S) and allowed to recover in oxygenated (95% O$_2$/5% CO$_2$) artificial cerebral spinal fluid (ACSF) containing 124 mM NaCl, 3 mM KCl, 24 mM NaHCO$_3$, 1.25 mM NaH$_2$PO$_4$, 2.0 mM CaCl$_2$, 1.0 mM MgSO$_4$, and 10 mM D-glucose; pH 7.3–7.4 for at least 1 h before recording.

2.5.1. Long-term potentiation (LTP)

Recordings for LTP were performed as previously reported (Foster et al., 2019). Field excitatory postsynaptic potentials (fEPSP) of the stratum radiatum of CA1 were recorded after stimulation (100 µs duration, every 20 s) of the Schaffer collaterals. Input-output curves (IO curve) were used for each slice to identify the stimulation intensity that evoked 50% the maximum response (approximately 0.2–0.3 mA). Five minutes after achieving a stable baseline, theta-burst stimulation (TBS) was used to induce LTP and recording continued for at least 30 min. The evoked peak fEPSP was normalized to baseline for analysis. Data was analyzed using Clampex 10.6 software (Molecular Devices). The average of each slice was used for statistical analysis.

2.5.2. Excitatory/inhibitory postsynaptic current (EPSC/IPSC)

Recordings for EPSC/IPSC were performed as previously reported (Kida et al., 2017). When recording, slices were placed into a recording chamber superfused (2 ml/min) with ACSF at 32 °C. Pyramidal neurons in CA1 were visualized with infrared optics using an upright fixed microscope equipped with a 40 × water-immersion lens (BX51WI, Olympus) and a digital camera (C11440, Hamamatsu). Patch pipettes were prepared with a horizontal pipette puller (P-97, Sutter Instruments) with a resistance of 4–6 MΩ and when recording, filled with intracellular solution containing 139 mM CsCl, 10 mM HEPES, 5 mM EGTA, 2 mM MgCl$_2$, 2 mM Mg ATP, 0.1 mM Na$_3$ GTP, 10 mM Glucose. In our protocol, the spontaneous excitatory postsynaptic currents (sEPSCs) and inhibitory postsynaptic currents (sIPSC) were sequentially recorded from the same neurons. After entering whole-cell mode, series resistance was corrected up to 60% if necessary. First, the sEPSC event was recorded for 5 min with holding potential at −70 mV. For recording sIPSC, the holding potential was set at 20 mV. For mEPSC and mIPSC recording, slices were bathed in tetrodotoxin (TTX, 0.5 μM) to block presynaptic action potentials and evoked neurotransmitter release. After giant postsynaptic currents (sEPSC and sIPSC) were completely inhibited, mEPSC and mIPSC were separately recorded for 5 min, respectively. Clampfit 10.7 software was used for EPSC and IPSC offline analysis. Firstly, a few typical mEPSC and mIPSC were selected to create the related templates, and then both templates were later used to search whole recording traces to generate amplitudes and frequency, respectively. The average of each neuron was used for statistical analysis.

2.6. Western blotting

Hippocampal tissues were homogenized in a 2 ml dounce tissue grinders (DWK Life Sciences, KT885300-0002) followed by sonication (Fisher Scientific, F60 Sonic Dismembrator). The protein concentration in the homogenate was determined by DCA methods (DC™ Protein Assay Kit I, Biorad, 5000111). The following primary antibodies were used: synaptophysin (1:2000), vGLUT1 (1:2000), PSD95 (1:2000), EAAT2 (1:20,000), GFAP (1:5000), actin (1:10,000), vGAT (1:2000), gephyrin (1:500), GABA$_A$ R α 1 (1: 500), and GAPDH (1:2000). All images were captured with ChemiDoc Imaging Systems (Bio-Rad) and analyzed with Image Lab software (Bio-Rad, V 5.2.1). The intensity for proteins of interest was normalized by the loading control (actin or GAPDH). Data were presented as percentage change relative to the sample from the control mouse.

2.7. Immunohistochemistry

Immunohistochemistry was performed as previously described (Knowland et al., 2017). Briefly, mice were intracardially perfused with ice-cold phosphate-buffered saline (PBS: 137 mM NaCl, 2.7 mM KCl, 10 mM Na$_2$HPO$_4$, 1.8 mM KH$_2$PO$_4$; PH = 7.4), post-fixed in 4% paraformaldehyde at 4 °C for 48 h, and then cryoprotected by immersion in 30% sucrose solution (in PBS with 0.02% sodium azide) for 24–48 h. Sagittal sections of 30 μm were sliced on a sliding microtome (Leica, SM2010R) and then stored in PBS with 0.02% sodium azide at 4 °C for further use,. The primary antibodies used were GFAP (1:1000), PV (1:1000) and DCX (1:500). Alexa Fluor 594 goat anti-mouse or anti-rabbit IgG was used as secondary antibodies (Invitrogen, A-11032 and A-11037, respectively, 1:500). All photographs (10× magnification, 890 μm × 667 μm) were captured by a fluorescence microscope (Zeiss, Axioskop 2 plus) with a 10 × objective (Zeiss Microscope Achroplan 10×/0.25 Objective, 440030), using AxioVision Rel. 4.8 software (Zeiss). For the quantitative evaluation of GFAP$^+$ cells, the GFAP$^+$ area was measured using ImageJ software (National Institutes of Health). For the quantitative evaluation of PV$^+$ and DCX$^+$ cells, the number of each positive cell was manually counted from the digital images acquired by the microscope. The average data of ≥6 slices (1 out of every 8 series slices) from each mouse was used for analysis.

2.8. Hippocampal microdialysis and glutamate measurement

Mice were anaesthetized under inhalation of isoflurane (5% for induction, 1–2% for maintenance) during the whole surgery. Micordialysis probes with 1 mm length of dialyzing membrane (Sci-pro, Mab 10.8.1 PES) and its guide cannula (Sci-pro, Mab.10.8.IC) were implanted in the CA1 region of hippocampus (anteroposterior = −2.0 mm, mediolateral = −1.9 mm, dorsoventral = −2.2 mm) and secured to the skull with anchor screw (Sci-pro, 4002002) (Sha et al., 2017) and dental glue (Prime dental, A2).

Sample collection was performed at least 36 h post-surgery. On the day of sample collection, microdialysis perfusion fluid (147 mM NaCl, 4 mM KCl, 1.2 mM CaCl$_2$, 1.2 mM MgCl$_2$; PH = 7.2–7.4) was used to wash out probes on free moving mice at a flow rate of 1.5 μl/min via a microinfusion pump (BASi, MD-1001), starting 2 h before and continuing during sample collection. A total of six samples (every 5 min) were collected per mouse.

For the analysis of glutamate concentration, an automated precolumn in-needle derivatization with o-phthaldialdehyde (OPA) and sulphite has been applied followed by a UHPLC separation by ALEXYS Neurotransmitter Analyzer based on DECADE II electrochemical detector with SenCell (Antec Scientific). A working potential of 850 mV (vs Ag/AgCl reference) and a range setting of 5 nA/V were used. The final chromatographic conditions for the analysis consisted of a Waters Acquity UPLC, HSS T3 column (50 × 1 mm i.d., 100 Å, 1.8 μm, Waters Corporation, 186003535). The mobile phase (solvent A) consisted of 50 mM phosphoric acid, 50 mM citric acid, and 0.1 mM EDTA; pH 3.1, 1.5% v/v acetonitrile was added prior to use. Solvent B, applied for post run cleanup of late eluting peaks, was the same mobile phase with 50% v/v acetonitrile. The system was operated at a flow rate of 200 μl/min at a pressure of 380 bar. The average glutamate concentration from each mouse was used for analysis.

2.9. ATP assay

The adenosine triphosphate (ATP) level was measured by ATP Assay Kit (Abcam, ab83355) according to manufacturer's instruction, which was based on the phosphorylation of glycerol in order to generate a product that can be easily quantified fluorometrically. Briefly, tissues were homogenized in 100 μl ice cold 2 N perchloric acid, diluted with 400 μl ATP buffer and then neutralized to PH = 6.5–8 by 2 M potassium hydroxide (KOH). Samples were then mixed with ATP reaction mix and incubated at room temperature for 30 min protected from light. The output was measured by a microplate reader (Molecular Devices, Spectramax M2) at wavelength of Excitation/Emission = 535/587 nm, and the data was normalized to percentage of control mice and then used for statistical analysis.

2.10. Statistical analysis

All statistical analyses were performed with GraphPad Prism 7.0 (GraphPad software, CA, USA). Outliers were identified and removed using ROUT method with Q value set a 1%. A one-way ANOVA comparison followed by uncorrected Fisher's LSD method for pairwise comparisons was used in Figs. 1, 6 and 7C, and 8. A one-sample *t*-test (hypothetical value = 100) was used to compare control with GWI/ vehicle in all Western bolt analysis (Figs. 1 and 7D–E) (Hong et al., 2016). A repeated measures ANOVA was used to analyze Fig. 4 (compare "before" with "after" or "before" with "stop" within GWI group) and Fig. S2. For the rest statistical analysis, a two-way ANOVA comparison followed by uncorrected Fisher's LSD method for pairwise comparisons was used. All data are represented as mean ± standard deviation (SD). *P < 0.05; **P < 0.01; ***P < 0.001. #P < 0.05; ##P < 0.01; ###P < 0.001.
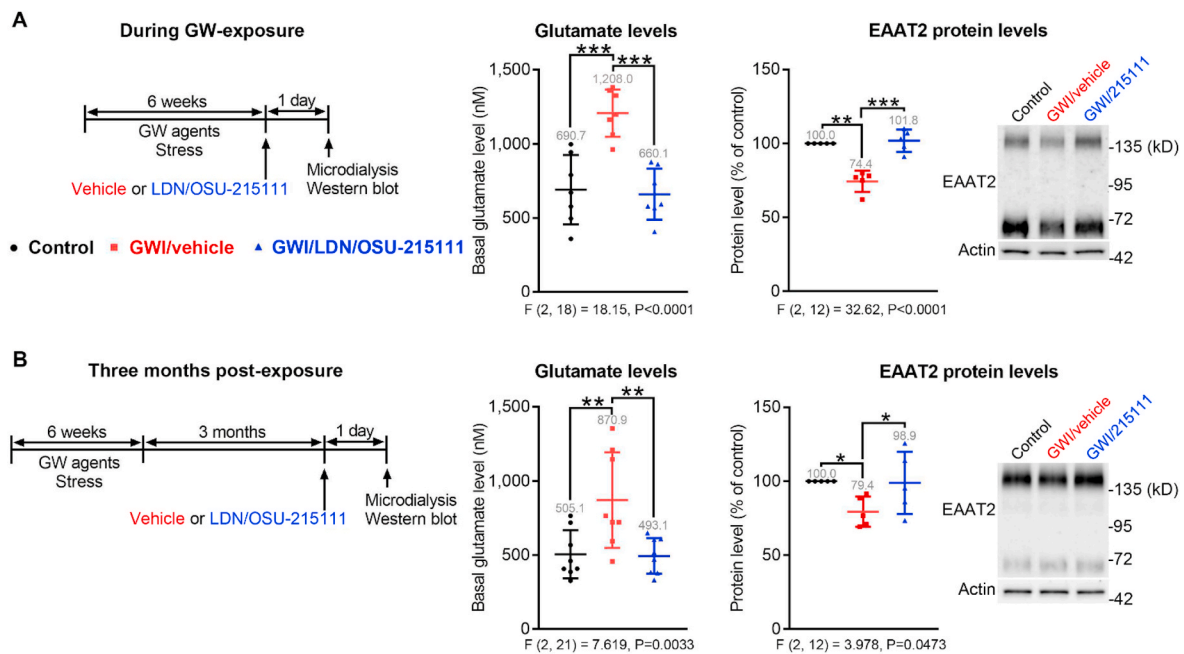
Fig. 1. GW-exposure causes elevated extracellular glutamate levels and decreased EAAT2 protein levels in the hippocampi, which can be normalized by LDN/OSU-215111. (A) During GW-exposure. (Left) Experimental procedure. Mice were randomly divided into three groups: control, GWI/vehicle, and GWI/LDN/OSU-215111. Both GWI/vehicle and GWI/LDN/OSU-215111 mice were exposed to GW agents and stress for six weeks. On the last day of exposure, mice received a single dose of LND/OSU-215111 (10 mg/kg) or vehicle. On the next day, extracellular glutamate levels in the hippocampal CA1 area were measured by microdialysis, and hippocampal EAAT2 protein levels were examined by Western blot analysis. GW-exposed mice exhibited elevated extracellular glutamate levels (middle, n = 7) and decreased EAAT2 levels (right, n = 5), which were normalized following LDN/OSU-215111 treatment. **(B)** At three-months post-exposure. (Left) Experimental procedure. At three-months post-exposure, mice received LND/OSU-215111 or vehicle. On the next day, extracellular glutamate levels and EAAT2 levels were measured. GW-exposed mice still exhibited elevated extracellular glutamate levels (middle, n = 8) and decreased EAAT2 levels (right, n = 5), which were normalized following LDN/OSU-215111 treatment. Data are presented as mean ± SD. Statistics are based on a one-way ANOVA followed by uncorrected Fisher's LSD method for pairwise comparisons. One-sample *t*-test (hypothetical value = 100) was used to compare control with GWI/vehicle in Western blot analysis. F and P values for one-way ANOVA are shown. *P < 0.05; **P < 0.01; ***P < 0.001.

3. Results

We first established a GWI model in mice as follows. Three-month-old C57BL/6J mice were exposed to GW-related agents and stress (GW-exposure) daily for six weeks. The GW agents and stress conditions applied in this study are described in the Method section. At three-months post-exposure, mice exhibited several GWI-like symptoms, including anxiety- and depression-like behavior, cognitive impairment, and fatigue. These symptoms were sustained for at least one-year post-exposure.

3.1. GWI mice exhibit elevated extracellular glutamate levels, which can be normalized by LDN/OSU-215111

As mentioned above, previous studies indicate that GW agents and stress can cause dysregulation of glutamate transmission. We investigated whether GWI mice exhibited elevated extracellular glutamate levels during the exposure and at three-months post-exposure. Microdialysis was employed to measure extracellular glutamate levels in the hippocampal CA1 area. This study was conducted as illustrated in Fig. 1. Littermate-matched mice were randomly divided into three groups: control (no GW-exposure, treated with vehicle), GWI/vehicle (GW-exposure, treated with vehicle), and GWI/LDN/OSU-215111 (GW-exposure, treated with LDN/OSU-215111). LDN/OSU-215111 or vehicle was given to the mice on the last day of exposure (Fig. 1 A) or at three-months post-exposure (Fig. 1 B); 10 mg/kg of LDN/OSU-215111 was used as in our previous study (Foster et al., 2019). *In vivo* microdialysis was conducted the next day. Results showed a significant increase in glutamate levels (~1.5–2 folds) in GWI/vehicle mice compared to control mice. Importantly, glutamate levels decreased following a single

dose of LDN/OSU-215111 treatment (Fig. 1 A). We previously demonstrated that LDN/OSU-215111 can rapidly up-regulate a subset of proteins in the perisynaptic astrocytic processes, including excitatory amino acid transporter 2 (EAAT2), via activation of local translation (Foster et al., 2018). We found that hippocampal EAAT2 protein levels decreased (~25%) in GWI/vehicle mice and significantly increased following a single dose of LDN/OSU-215111 (Fig. 1 A). Notably, at three-months post-exposure, glutamate levels in the exposed mice were still significantly higher than that in control mice and were decreased by LDN/OSU-215111 (Fig. 1 B). Hippocampal EAAT2 protein levels remained lower level in GWI/vehicle mice and was restored by LDN/OSU-215111 (Fig. 1 B). These results suggest that GW-exposure causes long-term glutamatergic abnormalities but appears amenable to intervention by LDN/OSU-215111.

3.2. LDN/OSU-215111 prevents the development of mood and cognitive deficits

We investigated whether normalizing extracellular glutamate levels by LDN/OSU-215111 could prevent the development of GWI. The experimental design of this study is illustrated in Fig. 2 A. Littermate-matched mice were randomly divided into three groups: control, GWI/vehicle, and GWI/LDN/OSU-215111. Since LDN/OSU-215111 at 10 mg/kg was able to normalize extracellular glutamate levels (Fig. 1), we used this dose in the study. Mice received either LDN/OSU-215111 or vehicle daily during and after six-week GW-exposure. Bodyweight was measured weekly. As shown in supplementary Fig. 1, GW-exposure significantly decreased bodyweight in the first week (5.31% decrease in males and 2.43% decrease in females). In male mice, significant bodyweight loss was observed during the entire eight-week recording period,
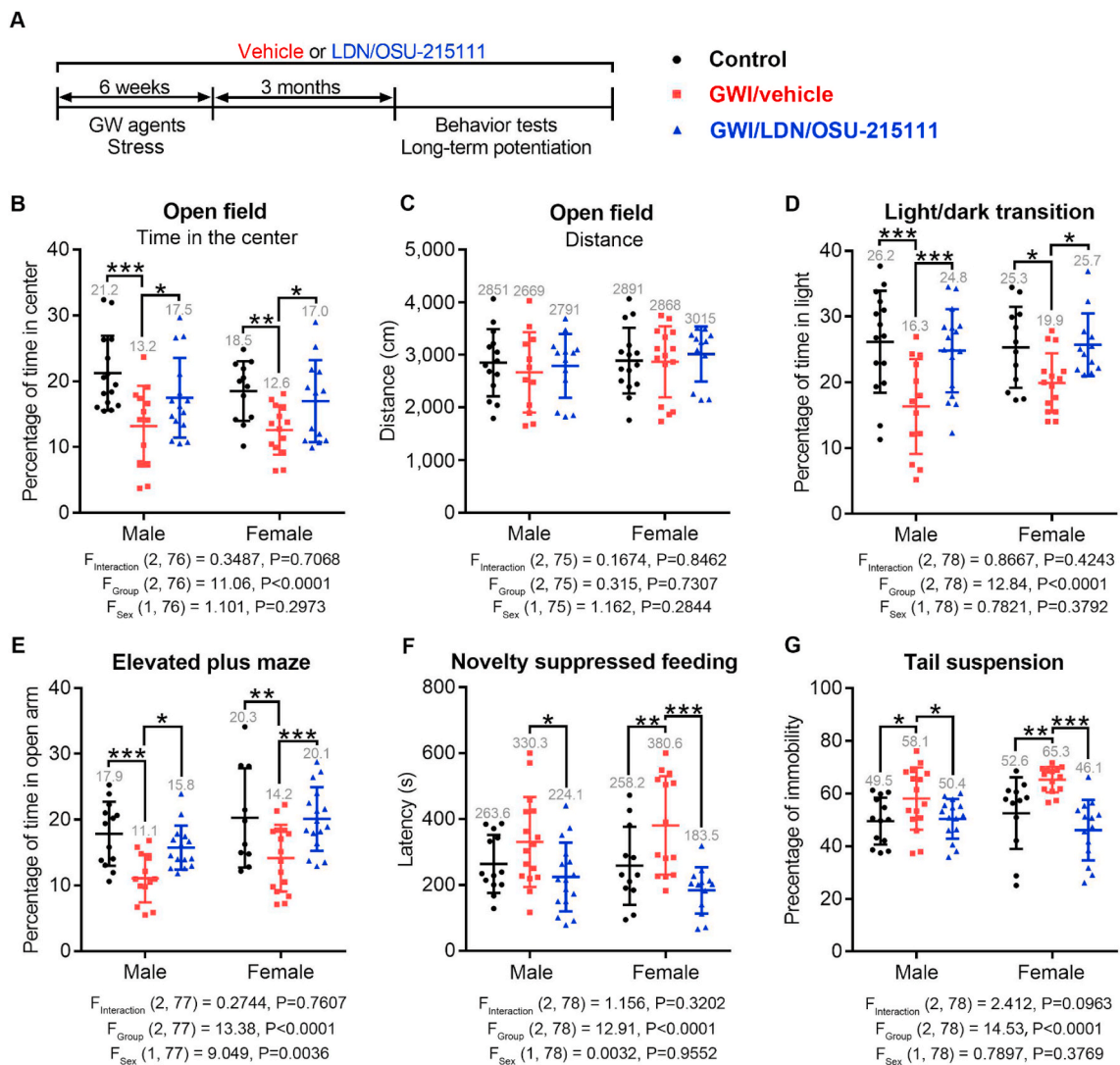
Fig 2. LDN/OSU-215111 prevents mood deficits in mice exposed to GW agents and stress. (A) Experimental procedure. Mice were randomly divided into three groups: control, GWI/vehicle, and GWI/LDN/OSU-215111. Both GWI/vehicle and GWI/LDN/OSU-215111 groups were exposed to GW agents and stress for six weeks. Mice received either vehicle or LDN/OSU-215111 daily during and after GW-exposure. Behavioral assessments were conducted three-months post-exposure. **(B–G)** Assessment of anxiety and depression by indicated five tests. Results of these tests indicated that GWI/vehicle mice developed anxiety- and depression-like behaviors. LDN/OSU-215111 treatment almost completely prevented these abnormalities. n = 15–18 males and n = 16–18 females each group. Data are presented as mean ± SD. Statistics are based on a two-way ANOVA comparison followed by uncorrected Fisher's LSD method for pairwise comparisons. F and P values for two-way ANOVA are shown. *P < 0.05; **P < 0.01; ***P < 0.001.

and this effect was partially prevented by treatment with LDN/OSU-215111 (Fig. S1 A). In female mice, significant bodyweight loss was only observed in the first week (Fig. S1 B).

At three-months post-exposure, mice were subjected to behavioral tests to assess mood and cognitive functions. Five tests were conducted to evaluate anxiety- and depressive-like behaviors, including open field, light/dark transition, elevated plus maze, novelty suppressed feeding, and tail suspension tests. Results showed that GWI/vehicle mice exhibited a significant decrease in the time spent in the center area, but not the total distance traveled in the open field test (Fig. 2B–C), a decrease in the light area in the light/dark transition test (Fig. 2 D), a decrease in the open arms in the elevated plus maze test (Fig. 2 E), an increase in the latency to the first bite of food in the novelty suppressed feeding test (Fig. 2 F), and an increase in the immobility time in the tail suspension test (Fig. 2 G), indicating the development of anxiety- and depression-like behaviors. Significantly, LDN/OSU-215111 treatment principally prevented development of these deficits (Fig. 2, B-G).

Next, we assessed cognitive functions by novel object recognition

test to assess recognitive long-term memory and Barnes maze test to assess spatial learning memory. Results of both tests indicated that cognitive functions were significantly impaired in male GWI/vehicle mice and declined (but not statistically significant) in female mice. Importantly, LDN/OSU-215111 treatment significantly prevented the development of cognitive deficits (Fig. 3A–D). Upon completion of behavioral assessments, a subset of mice was euthanized to analyze long-term potentiation (LTP) changes in the hippocampal CA3-CA1 circuit along the Schaffer collateral pathway. Male GWI/vehicle mice exhibited significant impairment of LTP, while LDN/OSU-215111 treatment completely prevented this impairment. No significant change of LTP was observed in female GWI/vehicle mice (Fig. 3E–F), which was consistent with the results of cognition tests (Fig. 3, A-C), suggesting that female mice may be more resilient to GW-exposure. Together, these data indicate that when treatment is introduced early on following GW-exposure, LDN/OSU-215111 effectively prevent mood and cognitive deficits.
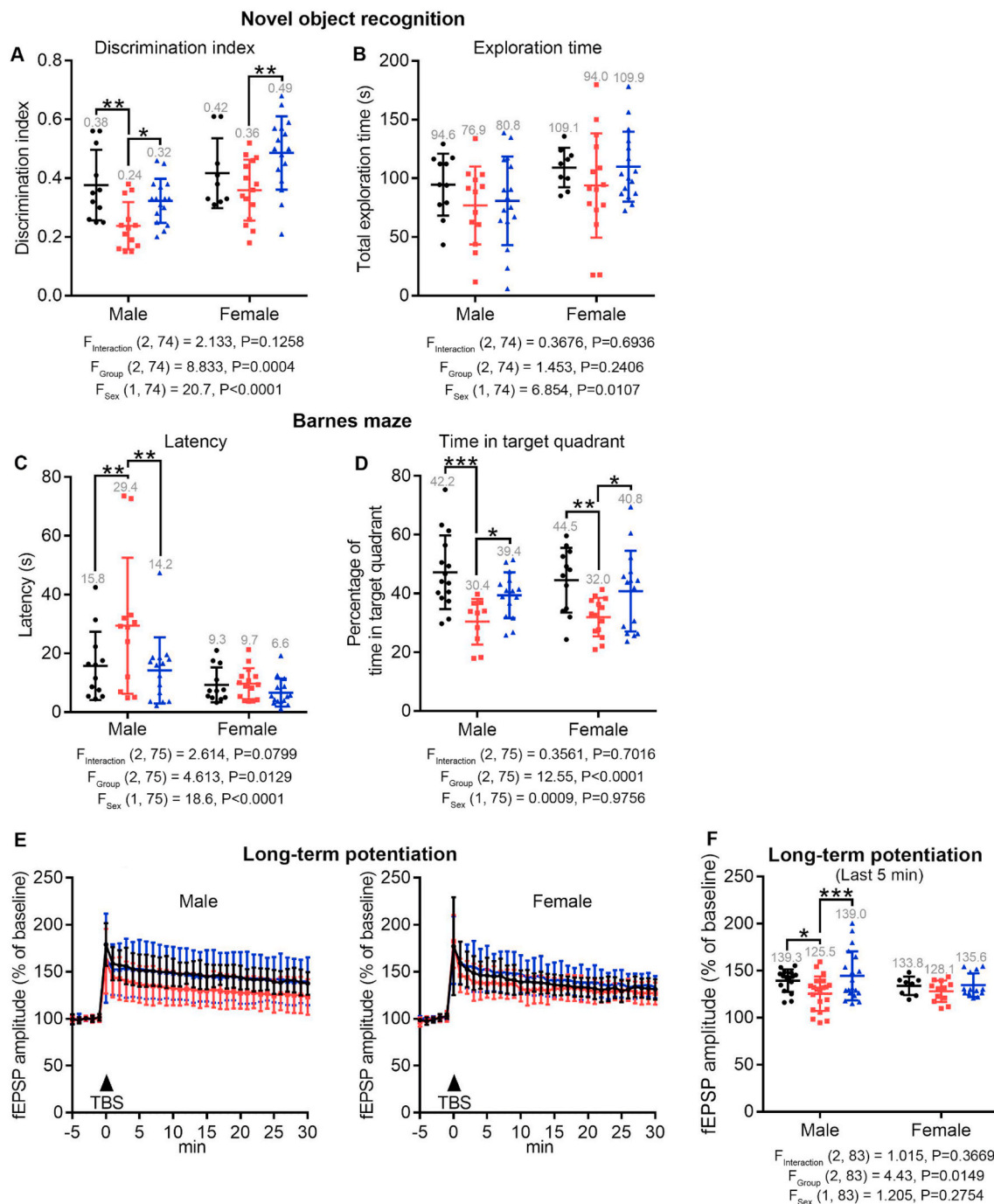
Fig. 3. LDN/OSU-215111 prevents cognitive deficits in mice exposed to GW agents and stress. Male GWI/vehicle mice showed a significant decrease in the time spent exploring the novel object, but not the total time of exploration in the novel object recognition test **(A–B)** and an increase in the latency to find the target hole and a decrease in the time spent in the target quadrant in the probe trial of Barnes maze test **(C–D)**, indicating memory deficits. LDN/OSU-215111 partially prevented these deficits. Female GWI/vehicle mice showed a decline (not statistically significant) in cognitive functions. n = 15–18 males and n = 16–18 females each group. **(E–F)** LTP assessment. Male GWI/vehicle mice showed a significant decrease in fEPSP LTP, and LDN/OSU-215111 treatment prevented the decrease. LTP was performed on CA1 apical dendrites. n = 16–24 sections, 5–7 mice per group. No significant difference was found in female mice. n = 8–13 sections, 4–7 mice per group. Data are presented as mean ± SD. Statistics are based on a two-way ANOVA comparison followed by uncorrected Fisher's LSD method for pairwise comparisons. F and P values for two-way ANOVA are shown. *P < 0.05; **P < 0.01; ***P < 0.001. TBS: theta-burst stimulation.

3.3. LDN/OSU-215111 normalizes mood and cognitive impairments after symptom onset

We investigated whether LDN/OSU-215111 could improve mood when symptoms were already present. The experimental design of this study is illustrated in Fig. 4 A. Littermate-matched mice were randomly divided into two groups: control (no GW-exposure) and GWI (GW-exposure). At five-months post-GW-exposure, mice were assessed for anxiety and depression by the behavioral tests mentioned above. GWI mice then received LDN/OSU-215111, and control mice received vehicle daily. After four-week of treatment, behavioral tests were conducted again to evaluate LDN/OSU-215111 effects. Results indicated that overall, GWI mice exhibited anxiety- and depression-like behaviors before treatment (Fig. 4, B–F; "Before"); following treatment, however,
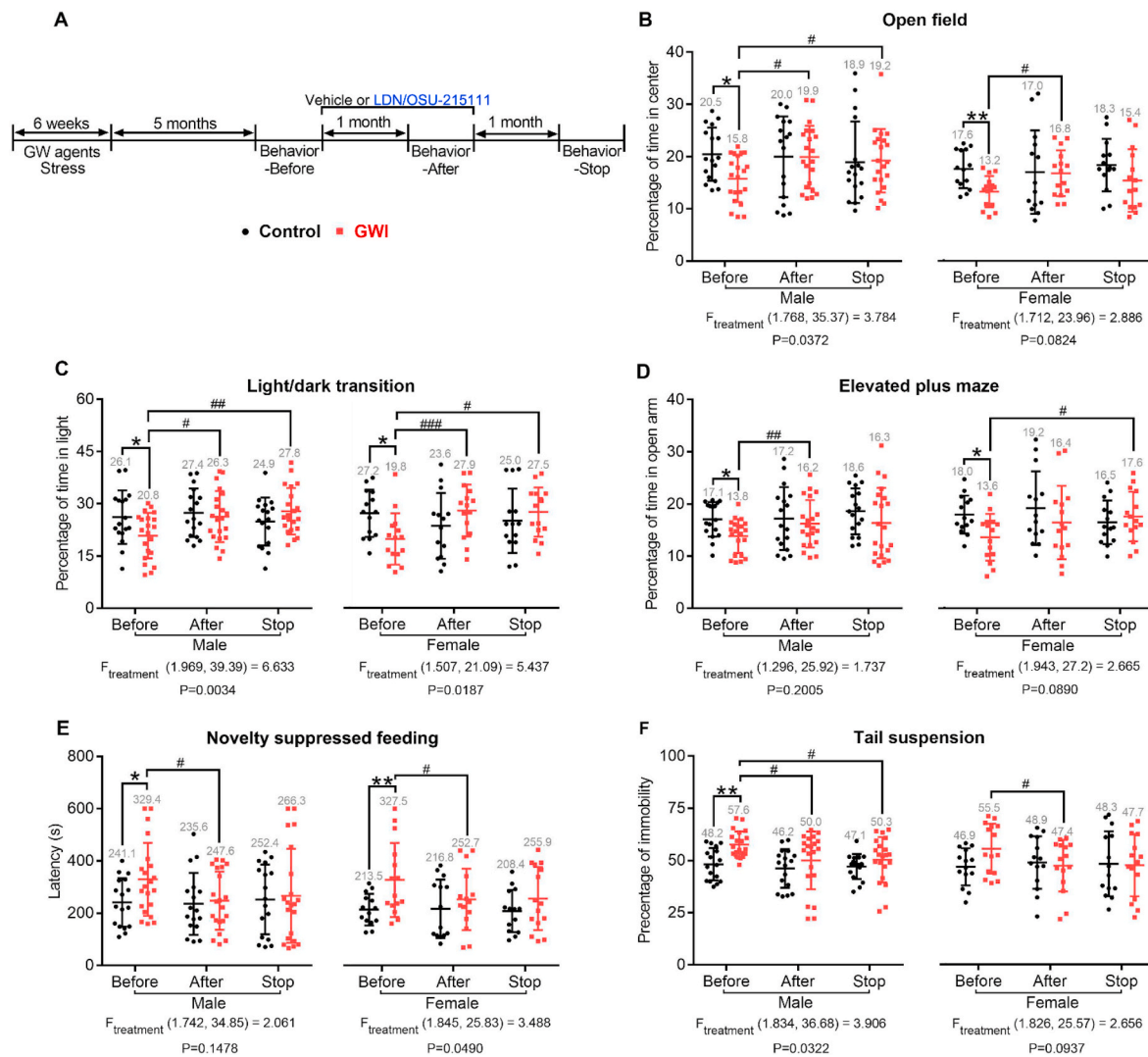
Fig. 4. LDN/OSU-215111 normalizes mood impairments after symptom onset. (A) Experimental procedure. Littermate-matched mice were randomly divided into two groups: control and GWI. GWI mice were exposed to GW agents and stress for six weeks. At five-months post-exposure, all mice were assessed for anxiety and depression ("before"). After the behavioral tests, GWI mice received LDN/OSU-215111, and control mice received vehicle. After one-month of treatment, behavioral tests were repeated ("after"). Following treatment cessation, behavioral tests were conducted again one-month later ("stop"). **(B–F)** Assessment of anxiety and depression. Overall, GWI mice exhibited anxiety- and depression-like behaviors before LDN/OSU-215111 treatment ("before"), and these behaviors significantly improved after the treatment ("after"). The effects of LDN/OSU-215111 lasted one month after treatment cessation ("stop"). The asterisk (*) indicates the difference between control and GWI mice, and the number sign (#) indicates the difference between "before" and "after", or "before" and "stop" in GWI mice. n = 17–21 males and n = 14–15 females each group. Data are presented as mean ± SD. Statistics are based on a two-way ANOVA comparison followed by uncorrected Fisher's LSD method for pairwise comparisons. A repeated measures ANOVA was used to compare "before" with "after", or "before" with "stop" within GWI group. F and P values for repeated measures ANOVA are shown. $F_{treatment}$ indicates the F value among "before, after and stop" within the GWI group. *P < 0.05; **P < 0.01. #P < 0.05; ##P < 0.01; ###P < 0.001.

these behaviors were significantly improved (Fig. 4, B–F; "After"). To investigate the duration and endurance of treatment, LDN/OSU-215111 administration was halted following all behavioral tests. One-month post-treatment cessation, behavioral tests were conducted again (Fig. 4 A). Notably, mice maintained anxiety- and depression-free behavior, only exhibiting a slight regression when compared to their performance immediately following treatment (Fig. 4, B–F; "Stop"), suggesting that the observed benefits are not palliative, and LDN/OSU-215111 may directly modify the disease. To confirm that the observed effects were not due to repeated testing, we analyzed the difference among "Before", "After", and "Stop" in the control group. Results showed no significant changes in the results of anxiety/depression tests (Fig. S2), indicating that repeated testing did not change the behavior.

We further investigated whether LDN/OSU-215111 treatment could improve cognitive functions at five months post-GW exposure, when the

chronic progression of the disease has been established. The experimental design of this study is illustrated in Fig. 5 A. The study included three groups: control, GWI/vehicle, and GWI/LDN/OSU-215111. At five-months post-GW-exposure, mice received either vehicle or LDN/OSU-215111 daily. After four-week of treatment, mice were assessed for cognitive functions by novel object recognition and Barnes maze tests. Results indicated that both male and female GWI/vehicle mice exhibited significant cognitive impairments. Importantly, LDN/OSU-215111 treatment significantly improved cognitive functions (Fig. 5B–E). Consistently, electrophysiological studies showed a significant reduction of LTP in GWI/vehicle mice, and LDN/OSU-215111 treatment significantly improved LTP (Fig. 5F–G). It is notable that cognitive functions in female GWI/vehicle mice declined only at three months post-exposure (Fig. 3) but were significantly impaired at six months post-exposure; in addition, male GWI/vehicle mice similarly
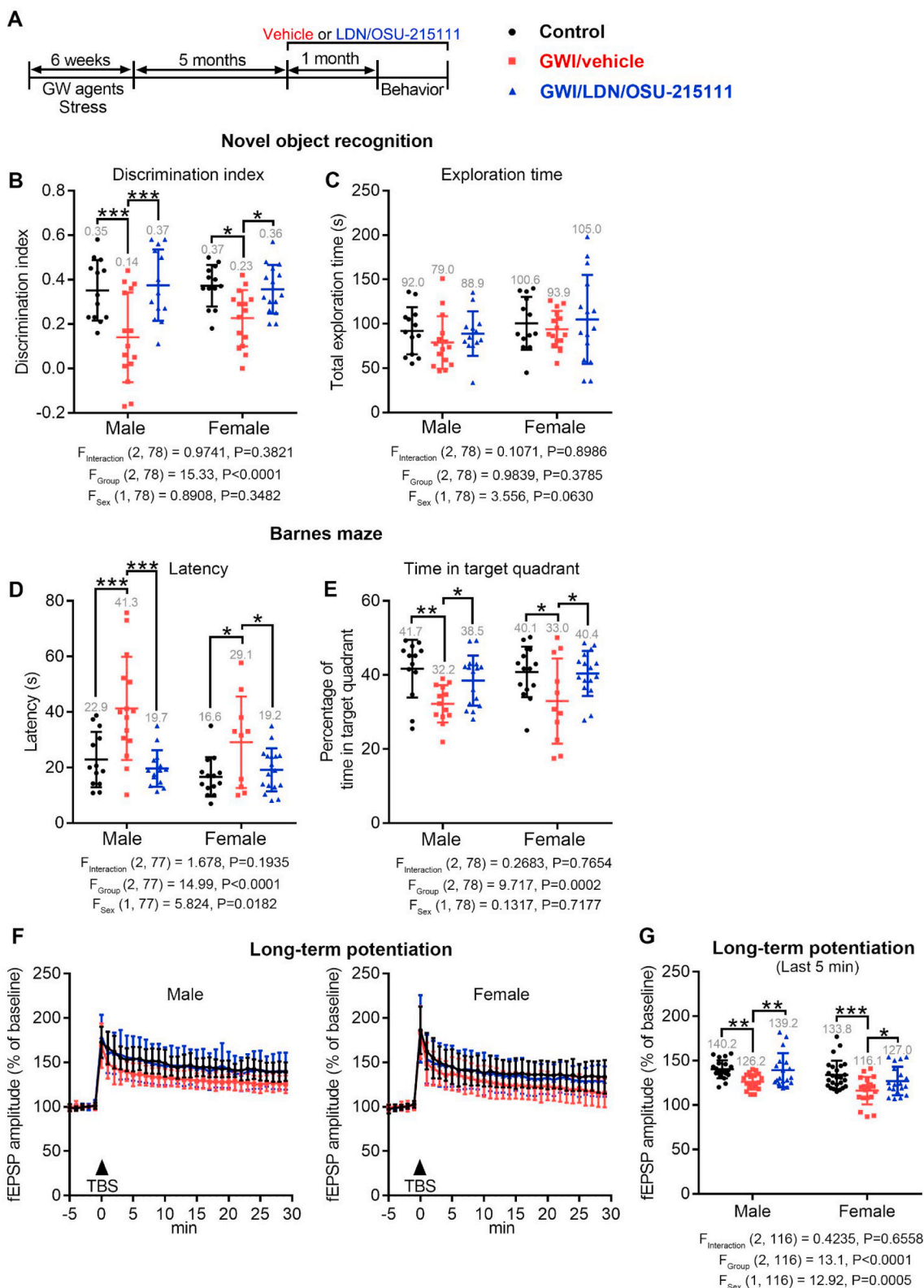
Fig. 5. LDN/OSU-215111 normalizes cognitive impairments at five months post-GW exposure. **(A)** Experimental procedure. Littermate-matched mice were randomly divided into three groups: control, GWI/vehicle, and GWI/LDN/OSU-215111. Both GWI/vehicle and GWI/LDN/OSU-215111 mice were exposed to GW agents and stress for six weeks. At five-months post-exposure, GWI/LDN/OSU-215111 mice received LDN/OSU-215111; control and GWI/vehicle mice received vehicle for one-month. Subsequently, behavioral tests were conducted. **(B–E)** Assessment of cognitive functions. Both male and female GWI/vehicle mice exhibited significant memory deficits. LDN/OSU-215111 treatment significantly improved cognitive functions. The probe trial results of Barnes Maze were presented in D-E. n = 16–25 males and n = 15–27 females each group. **(F–G)** LTP assessment. GWI/vehicle mice showed a significant decrease in fEPSP LTP, and LDN/OSU-215111 treatment normalized LTP. LTP was performed on CA1 apical dendrites. n = 18–21 sections, 4–7 mice per group for males; n = 19–25 sections, 4–5 mice per group for females. Data are presented as mean ± SD. Statistics are based on a two-way ANOVA comparison followed by uncorrected Fisher's LSD method for pairwise comparisons. F and P values for two-way ANOVA are shown. *P < 0.05; **P < 0.01; ***P < 0.001.
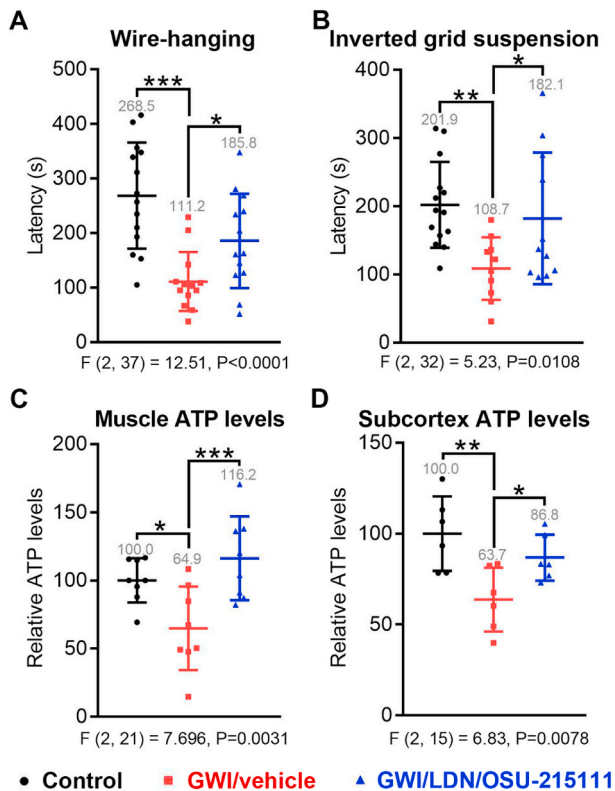
Fig. 6. GW-exposure causes fatigue and decreased total ATP levels, which can be improved by LDN/OSU-215111. Upon completion of the behavioral assessments in Fig. 5, a subset of mice were assessed for neuromuscular strength by wire-hanging (**A**) and inverted grid suspension (**B**) tests. n = 5–8 males and n = 6–7 females each group. GWI/vehicle mice exhibited reduced muscular strength, which was improved by LDN/OSU-215111 treatment (**A and B**). After the tests, mice were euthanized to measure total ATP levels in limb skeletal muscles (**C**, n = 8) and subcortex (**D**, n = 6). GWI/vehicle mice exhibited decreased total ATP levels in both tissues, which were normalized by LDN/OSU-215111 treatment (**C and D**). Data are presented as mean ± SD. Statistics are based on a one-way ANOVA followed by uncorrected Fisher's LSD method for pairwise comparisons. F and P values for one-way ANOVA are shown. *P < 0.05; **P < 0.01; ***P < 0.001.

demonstrated greater impairment at six months post-exposure. This suggests that the disease worsens with age. Taken together, these behavioral data indicate that when symptoms were already present, LDN/OSU-215111 still effectively improved mood and cognitive deficits.

3.4. GWI mice exhibit fatigue, which can be improved by LDN/OSU-215111

Fatigue is one of the most prevalent and debilitating symptoms affecting GW veterans (Kang et al., 2003; Kipen et al., 1999). We conducted wire-hanging and inverted grid suspension tests to evaluate neuromuscular strength. Results showed that hang time significantly decreased in GWI/vehicle mice, suggesting that mice had muscle fatigue/weakness; importantly, hang time increased with LDN/OSU-215111 treatment (Fig. 6A–B). Mitochondrial dysfunction is considered an underlying mechanism of chronic fatigue syndrome (Kodali et al., 2018; Shetty et al., 2017; Zakirova et al., 2017). We assessed limb skeletal muscle mitochondrial function by measuring total ATP levels. Consistently, total ATP levels were significantly decreased in GWI/vehicle mice and restored in GWI/LDN/OSU-215111 mice (Fig. 6 C). The subcortical brain regions, such as basal ganglia and thalamus, have been implicated in peripheral fatigue and also central fatigue

(Chaudhuri and Behan, 2000; Hou et al., 2016; Miller et al., 2014; Nakagawa et al., 2016). We found that total ATP levels were also significantly decreased in the subcortical brain regions of GWI/vehicle mice and partially restored in GWI/LDN/OSU-215111 mice (Fig. 6 D). The observed decreased ATP levels could be a major contributing factor to central fatigue that is reported in GW veterans (Wylie et al., 2019). This central fatigue could potentially contribute to muscle weakness (Marcora et al., 2009).

3.5. GW-exposure causes hippocampal abnormalities, which can be normalized by LDN/OSU-215111

Upon completion of behavioral assessments, mice were euthanized for further pathological or electrophysiological studies. We conducted immunohistochemical staining using (I) neuronal nuclei (NeuN) antibodies to examine hippocampal pyramidal neurons, (II) glial fibrillary acidic protein (GFAP) antibodies to examine astrocytes, (III) ionized calcium binding adaptor molecule 1 (Iba1) antibodies to examine microglia, (IV) parvalbumin (PV) antibodies to examine GABAergic interneurons, and (V) doublecortin (DCX) antibodies to examine newborn neurons. We did not observe significant changes for pyramidal neurons and microglia regarding the number, morphology, and signal intensity among the three groups. However, we observed significant changes for the following cell types in GWI/vehicle mice: (I) astrocytes - reduced the area of GFAP-positive (GFAP[+]) elements (cell body as well as processes; Fig. 7 A), suggesting astrocytic atrophy; (II) PV-positive (PV[+]) interneurons - reduced number (Fig. 7 B), suggesting loss of parvalbumin-positive interneurons; (III) DCX-positive (DCX^{+}) newborn neurons - reduced number (Fig. 7 C), suggesting decreased neurogenesis (Parihar et al., 2013). Importantly, LDN/OSU-215111 treatment significantly improved these deficits. We further examined expression levels of the following proteins in hippocampi by Western blot analysis, including (I) synaptophysin and vesicular glutamate transporter 1 (vGLUT1), which are located at the presynaptic terminals of glutamatergic neurons, (II) postsynaptic density protein 95 (PSD95), which is located at the post-synaptic terminals of glutamatergic neurons, (III) vesicular GABA transporter (vGAT), which is located at the presynaptic terminals of GABAergic interneurons, (IV) gephyrin and GABA$_A$ receptors, which are located at the postsynaptic terminals of GABAergic interneurons, and (V) EAAT2 and GFAP, which are located at astrocytes. Results showed that levels of these proteins, except gephyrin and GABA$_A$ receptors, were significantly decreased in GWI/vehicle mice and restored following LDN/OSU-215111 treatment (Fig. 7, D-E). Taken together, these results —including impaired glutamatergic synapses, astrocyte atrophy, loss of interneurons, and decreased neurogenesis— suggest that GW-exposure causes long-term hippocampal atrophy, which is reported in GW veterans (Apfel et al., 2011; Chao et al., 2017; Vythilingam et al., 2005). Importantly, this appears reversible by LDN/OSU-215111.

3.6. LDN/OSU-215111 normalizes excitatory and inhibitory synaptic transmission deficits

Next, we conducted whole-cell patch clamp recordings to assess synaptic transmission in CA1 pyramidal neurons. We measured glutamatergic synaptic transmission by recording both spontaneous and miniature excitatory postsynaptic currents (sEPSC and mEPSC). Results showed increases in sEPSC amplitude but decreases in mEPSC amplitude in GWI/vehicle mice (Fig. 8A–B). Increased sEPSC amplitude likely results from the increased tone of excitatory transmission as indicated by elevated extracellular glutamate levels described above (Fig. 1 B), and decreased mEPSC amplitude suggests reduced postsynaptic strength and/or number, which is consistent with decreased levels of PSD95 described above (Fig. 7 D). The frequencies of both sEPSC and mEPSC were decreased in GWI/vehicle mice (Fig. 8A–B). This suggests a reduction in the pre-synaptic glutamate release and/or the number of functional synapses, which is consistent with decreased levels of
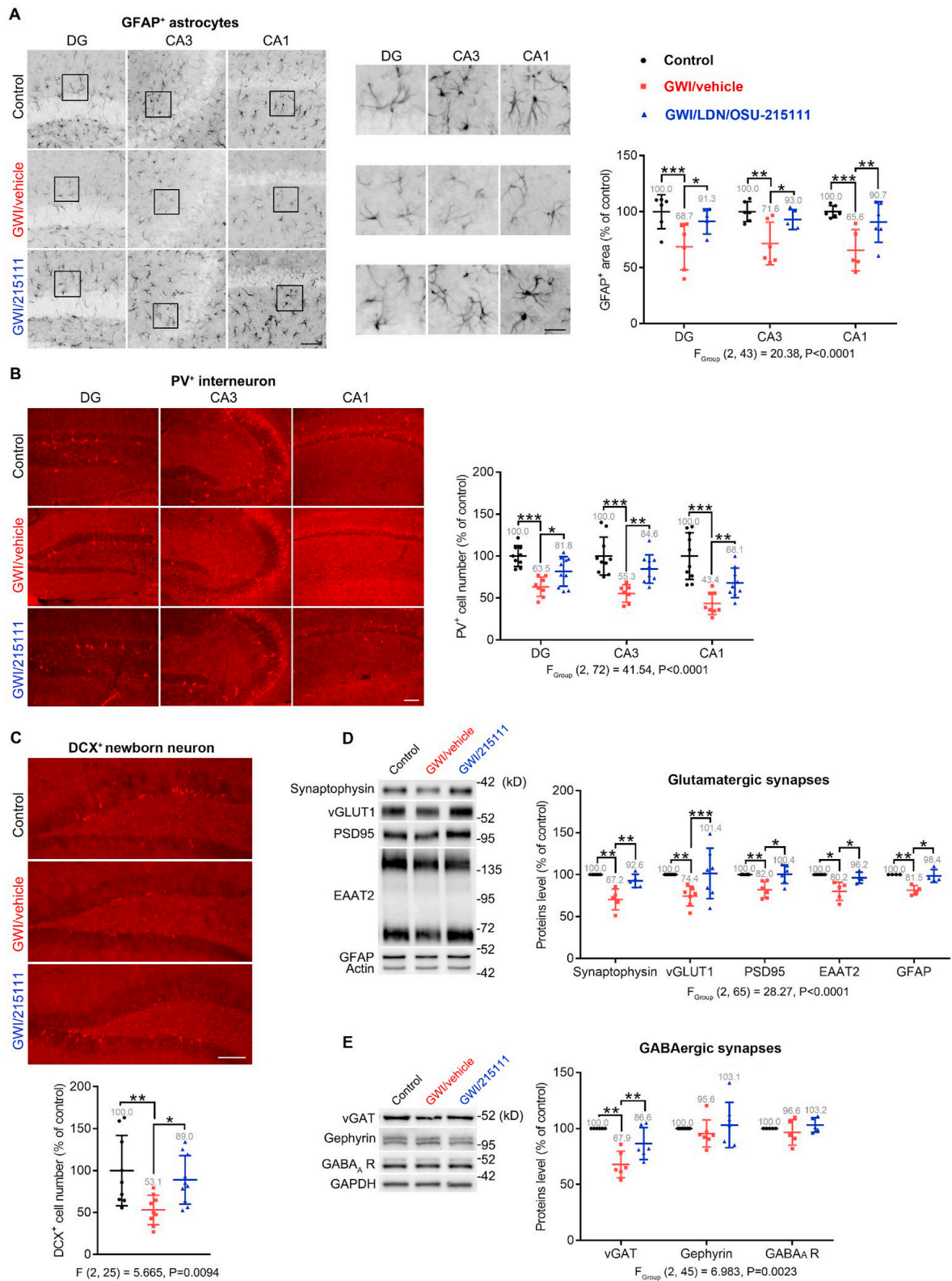
(caption on next page)

Fig. 7. GW-exposure causes impaired glutamatergic synapses, astrocyte atrophy, loss of interneurons, and decreased neurogenesis, which can be restored by LDN/OSU-215111. Upon completion of the behavioral assessments in Fig. 5, a subset of mice was euthanized for the following pathological studies. **(A)** GFAP immunohistochemical staining to examine astrocytes. Representative images are shown (scale bars: 100 μm). Boxed areas are shown enlarged in the middle column (scale bars: 25 μm). Quantitative analysis indicates that the GFAP[+] area decreased in GWI/vehicle mice and was partially restored in LDN/OSU-215111 treated mice. Data was generated from the percentage of GFAP staining in 890 μm × 667 μm area and normalized by control. n = 5–6 animals per group; average of ≥6 sections per animal. **(B)** Parvalbumin immunohistochemical staining to examine parvalbumin-expressing interneurons. Representative images are shown (scale bars: 100 μm). Quantitative analysis indicates that the number of PV[+] interneurons decreased in GWI/vehicle mice and was partially restored in LDN/OSU-215111 treated mice. n = 9–10 animals per group; average of ≥6 sections per animal. **(C)** Doublecortin immunohistochemical staining to examine newborn neurons in the dentate gyrus. Representative images are shown (scale bars: 100 μm). Quantitative analysis indicates that the number of DCX^{+} cells decreased in GWI/vehicle mice and was partially restored in LDN/OSU-215111 treated mice. n = 9–10 animals per group; average of ≥6 sections per animal. **(D–E)** Western blot analysis of hippocampal lysates to examine expression levels of indicated synaptic and astrocytic proteins. Representative immunoblots are shown. Quantitative analysis indicates that levels of the indicated proteins, except gephyrin and GABA$_A$ receptors, were significantly decreased in GWI/vehicle mice and restored in LDN/OSU-215111 treated mice. n = 4–7 mice per group. Data are presented as mean ± SD. Statistics are based on a two-way ANOVA **(A, B, D, E)** or one-way ANOVA **(C)** followed by uncorrected Fisher's LSD method for pairwise comparisons. One-sample *t*-test (hypothetical value = 100) was used to compare control with GWI/vehicle **(D, E)**. F and P values for one-way **(C)** or two-way **(A, B, D, E)** ANOVA are shown. *P < 0.05; **P < 0.01; ***P < 0.001. DG: dentate gyrus; CA: cornu ammonis; GFAP: glial fibrillary acidic protein; PV: parvalbumin; DCX: doublecortin.
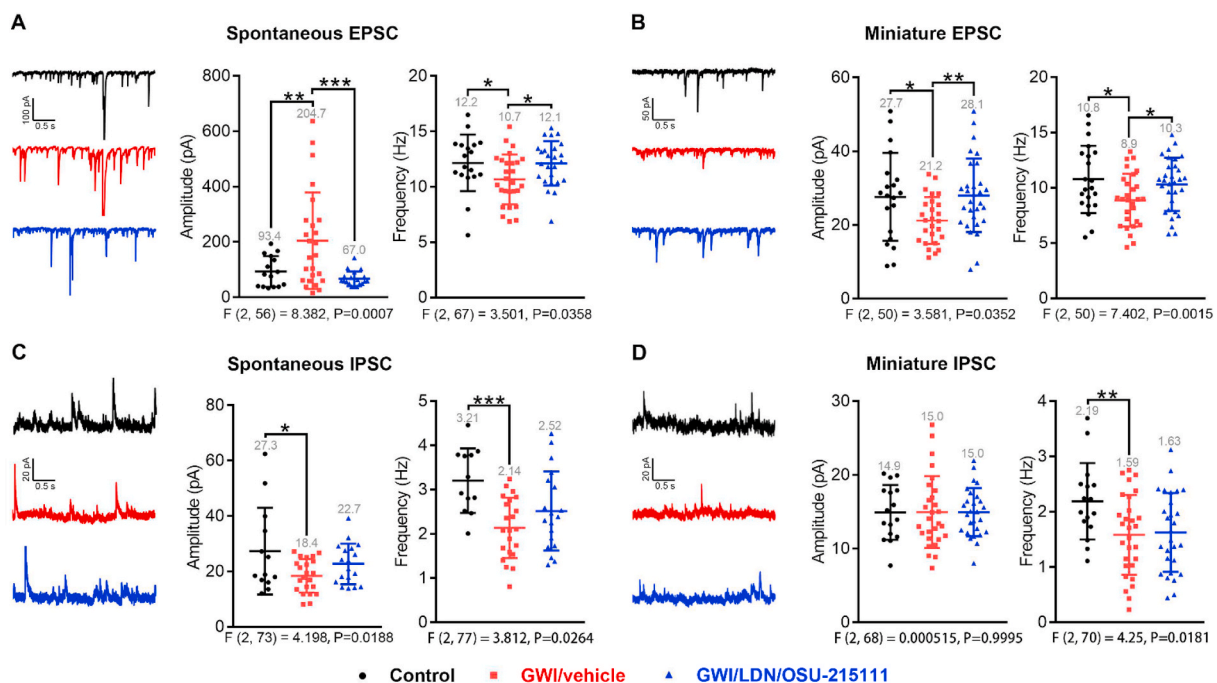
Fig. 8. GW-exposure causes impaired excitatory and inhibitory synaptic transmissions in CA1 pyramidal neurons, which can be partially restored by LDN/OSU-215111. Upon completion of the behavioral assessments in Fig. 5, a subset of mice were euthanized for conducting whole-cell patch clamp recordings to assess synaptic transmission in CA1 pyramidal neurons. **(A)** Spontaneous excitatory postsynaptic currents (sEPSC). Representative sEPSC traces are shown. Quantitative analysis shows increased amplitude but decreased frequency of sEPSC in GWI/vehicle mice, and both were restored by LDN/OSU-215111. n = 16–27 neurons, 7–10 mice per group. **(B)** Miniature excitatory postsynaptic currents (mEPSC). Representative mEPSC traces are shown. Quantitative analysis shows decreased amplitude and frequency of mEPSC in GWI/vehicle mice, and both were restored by LDN/OSU-215111. n = 19–31 neurons, 7–10 mice per group. **(C)** Spontaneous inhibitory postsynaptic currents (sIPSC). Representative sIPSC traces are shown. Quantitative analysis shows decreased amplitude and frequency of sIPSC in GWI/vehicle mice, which was partially restored (not statistically significant) by LDN/OSU-215111. n = 12–22 neurons, 7–10 mice per group. **(D)** Miniature inhibitory postsynaptic currents (mIPSC). Representative mIPSC traces are shown. Quantitative analysis shows similar amplitude but decreased frequency of mIPSC in GWI/vehicle mice, which was not restored by LDN/OSU-215111. n = 16–29 neurons, 7–10 mice per group. Data are presented as mean ± SD. Statistics are based on a one-way ANOVA comparison followed by uncorrected Fisher's LSD method for pairwise comparisons. F and P values for one-way ANOVA are shown. *P < 0.05; **P < 0.01; ***P < 0.001.

synaptophysin and vGLUT1 described above (Fig. 7 D). We further measured GABAergic synaptic transmission by recording both spontaneous and miniature inhibitory postsynaptic currents (sIPSC and mIPSC). Results showed decreases in sIPSC amplitude but no change in mIPSC amplitude in GWI/vehicle mice (Fig. 8C–D). Decreased sIPSC amplitude likely results from the loss of PV[+] interneurons described above (Fig. 7B), and no change in mIPSC amplitude is consistent with unchanged levels of gephyrin and GABA$_A$ receptor described above (Fig. 7E). The frequencies of both sIPSC and mIPSC were decreased in GWI/vehicle mice (Fig. 8C–D). This is likely due to loss of PV[+] interneurons (Fig. 7 B). Taken together, these results suggest that GW-

exposure impairs both the excitatory and inhibitory synaptic transmission in CA1 pyramidal neurons, which may contribute to mood and cognitive deficits. Importantly, LDN/OSU-215111 effectively normalized the excitatory deficit.

4. Discussion

In the present study, we found that GW-exposure causes long-term abnormalities in the hippocampi of mice, including increased basal extracellular glutamate concentrations, impaired structural integrity and function of glutamatergic synapses, astrocyte atrophy, decreased

numbers of parvalbumin interneurons, reduced numbers of newborn neurons, and altered excitatory and inhibitory synaptic transmission (Fig. 9). These hippocampal abnormalities may result in or contribute to the observed mood and cognitive deficits (Figs. 2–5). Importantly, LDN/OSU-215111 was able to effectively normalize hippocampal abnormalities and behavioral deficits.

As mentioned above, studies have shown that GW agents and stress can cause an increase in glutamate release from hippocampal neurons (Macht et al., 2020). We demonstrate for the first time *in vivo* that extracellular glutamate levels in the hippocampal CA1 of GW-exposed mice were significantly elevated (Fig. 1). This occurred not only during GW exposure, but also at three-months post-GW-exposure, suggesting alternations in glutamate homeostasis, i.e. the interplay between glutamate release and glutamate clearance, after chronic exposure. The observed decreased EAAT2 protein levels (Fig. 1) may contribute to elevated glutamate levels. Our electrophysiological results showing increased sEPSC amplitude (Fig. 8 A) also suggest elevated extracellular glutamate levels. Literature indicate that long-term glutamate dyshomeostasis can result in impairment of synaptic plasticity, alternation of excitatory and inhibitory transmission, and even synaptic loss (Talantova et al., 2013; Van Elst et al., 2014; Yuen et al., 2012). These damages were observed in the present study (Figs. 7 and 8).

Astrocytes play a critical role in the regulation of glutamate homeostasis (Coulter and Eid, 2012). It has been reported that chronic stress can cause atrophy of astrocytic process length, branching, and volume (Tynan et al., 2013). In addition, studies in mouse models of Alzheimer's disease demonstrated progressive astrocytic atrophy with decreased GFAP staining in the hippocampus in the early stage of the disease (Beauquis et al., 2013; Yeh et al., 2011). We observed similar astrocytic atrophy in this study (Fig. 7 A). Astrocytic deficits can result in decreased glutamate clearance and other functions, leading to impaired glutamatergic synapses.

Activity-dependent regulation controls the balance of synaptic excitation and inhibition in neural circuits, and disruption of this regulation impairs learning/memory and mood (Bateup et al., 2013; Lee et al., 2015, 2018; Wallace et al., 2012). PV interneurons play an important role in the balance of excitation and inhibition (Ferguson and Gao, 2018; Filice et al., 2016; Wohr et al., 2015). We found a significant reduction in PV interneurons in the hippocampus of GWI mice (Fig. 7 B), which is consistent with a previous report in a rat model of GWI (Megahed et al., 2014). Loss of PV interneurons likely contributes to impaired excitatory and inhibitory synaptic transmission as observed in our electrophysiological studies (Fig. 8). Furthermore, neuronal activity, especially the balance between glutamatergic and GABAergic inputs

regulate adult hippocampal neurogenesis (Sun et al., 2009; Zhao et al., 2008). PV interneurons play a critical role in maintaining neurogenesis (Song et al., 2013); loss of PV interneurons may contribute to decreased neurogenesis (Fig. 7 C).

The most striking finding in this study is that LDN/OSU-215111 has preventive and therapeutic potential for GWI (Figs. 2–6). LDN/OSU-215111 effectively normalizes hippocampal deficits, including impaired glutamatergic synapses, astrocyte atrophy, loss of interneurons, and decreased neurogenesis (Figs. 7 and 8). As mentioned above, our studies on the mechanism of action reveal that LDN/OSU-215111 can strengthen the structure and function of both the astrocytic processes and the glutamatergic synapses that together form the tripartite synapses (Foster et al., 2018). This explains how LDN/OSU-215111 normalizes behavioral and hippocampal deficits in GWI mice. Several studies have demonstrated reduced hippocampal volume and hippocampal dysfunction in veterans with GWI (Apfel et al., 2011; Chao et al., 2017; Vythilingam et al., 2005). Thus, restoration of tripartite glutamatergic synapses by LDN/OSU-215111 is a potential therapy for GWI. Given LDN/OSU-215111's capacity to restore multiple hippocampal deficits, it could have application to other diseases, such as post-traumatic stress disorder (PTSD) (Bonne et al., 2008; Bremner et al., 2003; Herrmann et al., 2012). LDN/OSU-215111 is an advanced small-molecule that has valuable drug-like properties. Continued development of this small-molecule series is currently under way.

Declaration of competing interest

The authors declare that they have no conflict of interest.

CRediT authorship contribution statement

Xueqin Wang: Conceptualization, Methodology, Validation, Investigation, Formal analysis, Data curation, Writing - original draft, Writing - review & editing, Visualization. **Zan Xu:** Validation, Investigation. **Fangli Zhao:** Validation, Investigation. **Kuanhung J. Lin:** Validation, Investigation. **Joshua B. Foster:** Methodology. **Tianqi Xiao:** Validation, Investigation. **Nydia Kung:** Validation, Investigation. **John P. Bruno:** Methodology. **Valentina Valentini:** Methodology, Investigation. **Kevin J. Hodgetts:** Resources. **Chien-liang Glenn Lin:** Conceptualization, Methodology, Resources, Writing - original draft, Writing - review & editing, Visualization, Supervision, Project administration, Funding acquisition.
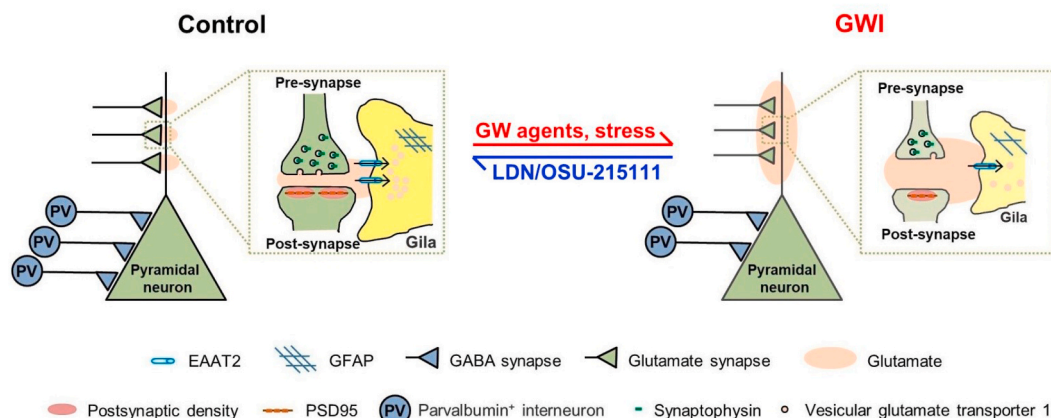

Fig. 9. A summary of the present research work. Left (control mice): Control mice have normal tripartite glutamatergic synapses and numbers of parvalbumin interneurons. Right (GW-exposed mice): GWI/vehicle mice exhibited increased basal extracellular glutamate concentrations, impaired structural integrity and function of glutamatergic synapses, reduced numbers of astrocytes, decreased numbers of parvalbumin interneurons, reduced numbers of newborn neurons, and altered excitatory and inhibitory synaptic transmission. LDN/OSU-215111 effectively normalizes hippocampal abnormalities and behavioral deficits.

Acknowledgements

Appendix A. Supplementary data

Supplementary data related to this article can be found at https://doi.org/10.1016/j.ynstr.2020.100240.

References

Abdel-Rahman, A., Abou-Donia, S., El-Masry, E., Shetty, A., Abou-Donia, M., 2004. Stress and combined exposure to low doses of pyridostigmine bromide, DEET, and permethrin produce neurochemical and neuropathological alterations in cerebral cortex, hippocampus, and cerebellum. J. Toxicol. Environ. Health Part A 67, 163–192.

Abdel-Rahman, A., Shetty, A.K., Abou-Donia, M.B., 2001. Subchronic dermal application of N,N-diethyl m-toluamide (DEET) and permethrin to adult rats, alone or in combination, causes diffuse neuronal cell death and cytoskeletal abnormalities in the cerebral cortex and the hippocampus, and Purkinje neuron loss in the cerebellum. Exp. Neurol. 172, 153–171.

Apfel, B.A., Ross, J., Hlavin, J., Meyerhoff, D.J., Metzler, T.J., Marmar, C.R., Weiner, M. W., Schuff, N., Neylan, T.C., 2011. Hippocampal volume differences in Gulf War veterans with current versus lifetime posttraumatic stress disorder symptoms. Biol. Psychiatr. 69, 541–548.

Bateup, H.S., Johnson, C.A., Denefrio, C.L., Saulnier, J.L., Kornacker, K., Sabatini, B.L., 2013. Excitatory/inhibitory synaptic imbalance leads to hippocampal hyperexcitability in mouse models of tuberous sclerosis. Neuron 78, 510–522.

Beauquis, J., Pavía, P., Pomilio, C., Vinuesa, A., Podlutskaya, N., Galvan, V., Saravia, F., 2013. Environmental enrichment prevents astroglial pathological changes in the hippocampus of APP transgenic mice, model of Alzheimer's disease. Exp. Neurol. 239, 28–37.

Bonne, O., Vythilingam, M., Inagaki, M., Wood, S., Neumeister, A., Nugent, A.C., Snow, J., Luckenbaugh, D.A., Bain, E.E., Drevets, W.C., Charney, D.S., 2008. Reduced posterior hippocampal volume in posttraumatic stress disorder. J. Clin. Psychiatr. 69, 1087–1091.

Bremner, J.D., Vythilingam, M., Vermetten, E., Southwick, S.M., McGlashan, T., Nazeer, A., Khan, S., Vaccarino, L.V., Soufer, R., Garg, P.K., Ng, C.K., Staib, L.H., Duncan, J.S., Charney, D.S., 2003. MRI and PET study of deficits in hippocampal structure and function in women with childhood sexual abuse and posttraumatic stress disorder. Am. J. Psychiatr. 160, 924–932.

Carreras, I., Aytan, N., Mellott, T., Choi, J.K., Lehar, M., Crabtree, L., Leite-Morris, K., Jenkins, B.G., Blusztajn, J.K., Dedeoglu, A., 2018. Anxiety, neuroinflammation, cholinergic and GABAergic abnormalities are early markers of Gulf War illness in a mouse model of the disease. Brain Res. 1681, 34–43.

Chao, L.L., Raymond, M.R., Leo, C.K., Abadjian, L.R., 2017. Evidence of hippocampal structural alterations in Gulf war veterans with predicted exposure to the khamisiyah plume. J Occupational Environ Med 59, 923–929.

Chaudhuri, A., Behan, P.O., 2000. Fatigue and basal ganglia. J. Neurol. Sci. 179, 34–42.

Colovic, M.B., Krstic, D.Z., Lazarevic-Pasti, T.D., Bondzic, A.M., Vasic, V.M., 2013. Acetylcholinesterase inhibitors: pharmacology and toxicology. Curr. Neuropharmacol. 11, 315–335.

Cory-Slechta, Deborah, Wedge, Roberta, 2016. Gulf war and health: volume 10: update of health effects of serving in the Gulf war, 2016, 10. National Academies Press.

Coulter, D.A., Eid, T., 2012. Astrocytic regulation of glutamate homeostasis in epilepsy. Glia 60, 1215–1226.

Duric, V., Banasr, M., Licznerski, P., Schmidt, H.D., Stockmeier, C.A., Simen, A.A., Newton, S.S., Duman, R.S., 2010. A negative regulator of MAP kinase causes depressive behavior. Nat. Med. 16, 1328–1332.

Ferguson, B.R., Gao, W.J., 2018. PV interneurons: critical regulators of E/I balance for prefrontal cortex-dependent behavior and psychiatric disorders. Front. Neural Circ. 12, 37.

Filice, F., Vörckel, K.J., Sungur, A.Ö., Wöhr, M., Schwaller, B., 2016. Reduction in parvalbumin expression not loss of the parvalbumin-expressing GABA interneuron subpopulation in genetic parvalbumin and shank mouse models of autism. Mol. Brain 9, 10.

Foster, J.B., Lashley, R., Zhao, F., Wang, X., Kung, N., Askwith, C.C., Lin, L., Shultis, M. W., Hodgetts, K.J., Lin, C.G., 2019. Enhancement of tripartite synapses as a potential therapeutic strategy for Alzheimer's disease: a preclinical study in rTg4510 mice. Alzheimer's Res. Ther. 11, 75.

Foster, J.B., Zhao, F., Wang, X., Xu, Z., Lin, K., Askwith, C.C., Hodgetts, K.J., Lin, C.G., 2018. Pyridazine-derivatives enhance structural and functional plasticity of tripartite synapse via activation of local translation in astrocytic processes. Neuroscience 388, 224–238.

Fulco, C.E., Liverman, C.T., Sox, H.C., 2000. Gulf War and health: volume 1. Depleted uranium, pyridostigmine bromide, sarin, and vaccines. National Academies Press.

Golomb, B.A., 2008. Acetylcholinesterase inhibitors and Gulf war illnesses. In: Proceedings of the National Academy of Sciences, vol. 105, pp. 4295–4300.

Gray, G.C., Reed, R.J., Kaiser, K.S., Smith, T.C., Gastañaga, V.M., 2002. Self-reported symptoms and medical conditions among 11,868 Gulf war-era veterans: the seabee health study. Am. J. Epidemiol. 155, 1033–1044.

Haley, R.W., Kurt, T.L., 1997. Self-reported exposure to neurotoxic chemical combinations in the Gulf War. A cross-sectional epidemiologic study. Jama 277, 231–237.

Hattiangady, B., Mishra, V., Kodali, M., Shuai, B., Rao, X., Shetty, A.K., 2014. Object location and object recognition memory impairments, motivation deficits and depression in a model of Gulf War illness. Front. Behav. Neurosci. 8, 78.

Herrmann, L., Ionescu, I.A., Henes, K., Golub, Y., Wang, N.X., Buell, D.R., Holsboer, F., Wotjak, C.T., Schmidt, U., 2012. Long-lasting hippocampal synaptic protein loss in a mouse model of posttraumatic stress disorder. PloS One 7, e42603.

Hong, S., Beja-Glasser, V.F., Nfonoyim, B.M., Frouin, A., Li, S., Ramakrishnan, S., Merry, K.M., Shi, Q., Rosenthal, A., Barres, B.A., Lemere, C.A., Selkoe, D.J., Stevens, B., 2016. Complement and microglia mediate early synapse loss in Alzheimer mouse models. Science 352, 712–716.

Hou, L.J., Song, Z., Pan, Z.J., Cheng, J.L., Yu, Y., Wang, J., 2016. Decreased activation of subcortical brain areas in the motor fatigue state: an fMRI study. Front. Psychol. 7, 1154.

Kang, H.K., Li, B., Mahan, C.M., Eisen, S.A., Engel, C.C., 2009. Health of US veterans of 1991 Gulf War: a follow-up survey in 10 years. J Occupational Environ Med 51, 401–410.

Kang, H.K., Natelson, B.H., Mahan, C.M., Lee, K.Y., Murphy, F.M., 2003. Post-traumatic stress disorder and chronic fatigue syndrome-like illness among Gulf War veterans: a population-based survey of 30,000 veterans. Am. J. Epidemiol. 157, 141–148.

Kassem, M.S., Lagopoulos, J., Stait-Gardner, T., Price, W.S., Chohan, T.W., Arnold, J.C., Hatton, S.N., Bennett, M.R., 2013. Stress-induced grey matter loss determined by MRI is primarily due to loss of dendrites and their synapses. Mol. Neurobiol. 47, 645–661.

Kida, H., Sakimoto, Y., Mitsushima, D., 2017. Slice patch clamp technique for analyzing learning-induced plasticity. JoVE : JoVE (129), e55876.

Kipen, H.M., Hallman, W., Kang, H., Fiedler, N., Natelson, B.H., 1999. Prevalence of chronic fatigue and chemical sensitivities in Gulf Registry Veterans. Archives Environ Health 54, 313–318.

Knowland, D., Lilascharoen, V., Pacia, C.P., Shin, S., Wang, E.H., Lim, B.K., 2017. Distinct ventral pallidal neural populations mediate separate symptoms of depression. Cell 170, 284–297 e218.

Kodali, M., Hattiangady, B., Shetty, G.A., Bates, A., Shuai, B., Shetty, A.K., 2018. Curcumin treatment leads to better cognitive and mood function in a model of Gulf War Illness with enhanced neurogenesis, and alleviation of inflammation and mitochondrial dysfunction in the hippocampus. Brain Behav. Immun. 69, 499–514.

Kong, Q., Chang, L.C., Takahashi, K., Liu, Q., Schulte, D.A., Lai, L., Ibabao, B., Lin, Y., Stouffer, N., Das Mukhopadhyay, C., Xing, X., Seyb, K.I., Cuny, G.D., Glicksman, M. A., Lin, C.L., 2014. Small-molecule activator of glutamate transporter EAAT2 translation provides neuroprotection. J. Clin. Invest. 124, 1255–1267.

Lee, J., Chung, C., Ha, S., Lee, D., Kim, D.-Y., Kim, H., Kim, E., 2015. Shank3-mutant mice lacking exon 9 show altered excitation/inhibition balance, enhanced rearing, and spatial memory deficit. Front. Cell. Neurosci. 9.

Lee, S., Lee, E., Kim, R., Kim, J., Lee, S., Park, H., Yang, E., Kim, H., Kim, E., 2018. Shank2 deletion in parvalbumin neurons leads to moderate hyperactivity, enhanced self-grooming and suppressed seizure susceptibility in mice. Front. Mol. Neurosci. 11, 209.

Leger, M., Quiedeville, A., Bouet, V., Haelewyn, B., Boulouard, M., Schumann-Bard, P., Freret, T., 2013. Object recognition test in mice. Nat. Protoc. 8, 2531–2537.

Li, N., Liu, R.J., Dwyer, J.M., Banasr, M., Lee, B., Son, H., Li, X.Y., Aghajanian, G., Duman, R.S., 2011. Glutamate N-methyl-D-aspartate receptor antagonists rapidly reverse behavioral and synaptic deficits caused by chronic stress exposure. Biol. Psychiatr. 69, 754–761.

Macht, V.A., Woodruff, J.L., Burzynski, H.E., Grillo, C.A., Reagan, L.P., Fadel, J.R., 2020. Interactions between pyridostigmine bromide and stress on glutamatergic neurochemistry: insights from a rat model of Gulf War Illness. Neurobiol Stress 12, 100210.

Marcora, S.M., Staiano, W., Manning, V., 2009. Mental fatigue impairs physical performance in humans. J. Appl. Physiol. 106, 857–864.

Megahed, T., Hattiangady, B., Shuai, B., Shetty, A.K., 2014. Parvalbumin and neuropeptide Y expressing hippocampal GABA-ergic inhibitory interneuron numbers decline in a model of Gulf War illness. Front. Cell. Neurosci. 8, 447.

Meyer, D.A., Shafer, T.J., 2006. Permethrin, but not deltamethrin, increases spontaneous glutamate release from hippocampal neurons in culture. Neurotoxicology 27, 594–603.

Miller, A.H., Jones, J.F., Drake, D.F., Tian, H., Unger, E.R., Pagnoni, G., 2014. Decreased basal ganglia activation in subjects with chronic fatigue syndrome: association with symptoms of fatigue. PloS One 9, e98156.

Musazzi, L., Milanese, M., Farisello, P., Zappettini, S., Tardito, D., Barbiero, V.S., Bonifacino, T., Mallei, A., Baldelli, P., Racagni, G., Raiteri, M., Benfenati, F., Bonanno, G., Popoli, M., 2010. Acute stress increases depolarization-evoked glutamate release in the rat prefrontal/frontal cortex: the dampening action of antidepressants. PloS One 5, e8566.

Nakagawa, S., Takeuchi, H., Taki, Y., Nouchi, R., Kotozaki, Y., Shinada, T., Maruyama, T., Sekiguchi, A., Iizuka, K., Yokoyama, R., 2016. Basal ganglia correlates of fatigue in young adults. Sci. Rep. 6, 21386.

Nettleman, M., 2015. Gulf war illness: challenges persist. Trans. Am. Clin. Climatol. Assoc. 126, 237–247.

Ojo, J.O., Abdullah, L., Evans, J., Reed, J.M., Montague, H., Mullan, M.J., Crawford, F.C., 2014. Exposure to an organophosphate pesticide, individually or in combination with other Gulf War agents, impairs synaptic integrity and neuronal differentiation, and is accompanied by subtle microvascular injury in a mouse model of Gulf War agent exposure. Neuropathology : Off J Jpn Soc Neuropathol 34, 109–127.

Parihar, V.K., Hattiangady, B., Shuai, B., Shetty, A.K., 2013. Mood and memory deficits in a model of Gulf War illness are linked with reduced neurogenesis, partial neuron loss, and mild inflammation in the hippocampus. Neuropsychopharmacology : Off Publ Am College Neuropsychopharmacol 38, 2348–2362.

Pavlovsky, L., Browne, R.O., Friedman, A., 2003. Pyridostigmine enhances glutamatergic transmission in hippocampal CA1 neurons. Exp. Neurol. 179, 181–187.

Raudensky, J., Yamamoto, B.K., 2007. Effects of chronic unpredictable stress and methamphetamine on hippocampal glutamate function. Brain Res. 1135, 129–135.

Serchov, T., van Calker, D., Biber, K., 2016. Light/dark transition test to assess anxiety-like behavior in mice. Bio-Protocol 6.

Sha, L., Wang, X., Li, J., Shi, X., Wu, L., Shen, Y., Xu, Q., 2017. Pharmacologic inhibition of Hsp90 to prevent GLT-1 degradation as an effective therapy for epilepsy. J. Exp. Med. 214, 547–563.

Shetty, G.A., Hattiangady, B., Upadhya, D., Bates, A., Attaluri, S., Shuai, B., Kodali, M., Shetty, A.K., 2017. Chronic oxidative stress, mitochondrial dysfunction, Nrf2 activation and inflammation in the Hippocampus accompany heightened systemic inflammation and oxidative stress in an animal model of Gulf war illness. Front. Mol. Neurosci. 10, 182.

Song, J., Sun, J., Moss, J., Wen, Z., Sun, G.J., Hsu, D., Zhong, C., Davoudi, H., Christian, K.M., Toni, N., Ming, G.L., Song, H., 2013. Parvalbumin interneurons mediate neuronal circuitry-neurogenesis coupling in the adult hippocampus. Nat. Neurosci. 16, 1728–1730.

Steele, L., Sastre, A., Gerkovich, M.M., Cook, M.R., 2012. Complex factors in the etiology of Gulf War illness: wartime exposures and risk factors in veteran subgroups. Environ. Health Perspect. 120, 112–118.

Sun, B., Halabisky, B., Zhou, Y., Palop, J.J., Yu, G., Mucke, L., Gan, L., 2009. Imbalance between GABAergic and glutamatergic transmission impairs adult neurogenesis in an animal model of Alzheimer's disease. Cell Stem Cell 5, 624–633.

Sunyer, B., Patil, S., Höger, H., Luber, G., 2007. Barnes maze, a useful task to assess spatial reference memory in the mice. Protocol Exchange 10.

Takahashi, K., Kong, Q., Lin, Y., Stouffer, N., Schulte, D.A., Lai, L., Liu, Q., Chang, L.C., Dominguez, S., Xing, X., Cuny, G.D., Hodgetts, K.J., Glicksman, M.A., Lin, C.L., 2015. Restored glial glutamate transporter EAAT2 function as a potential therapeutic approach for Alzheimer's disease. J. Exp. Med. 212, 319–332.

Talantova, M., Sanz-Blasco, S., Zhang, X., Xia, P., Akhtar, M.W., Okamoto, S.-i., Dziewczapolski, G., Nakamura, T., Cao, G., Pratt, A.E., 2013. Aβ induces astrocytic glutamate release, extrasynaptic NMDA receptor activation, and synaptic loss. Proc. Natl. Acad. Sci. Unit. States Am. 110, E2518–E2527.

Toomey, R., Alpern, R., Vasterling, J.J., Baker, D.G., Reda, D.J., Lyons, M.J., Henderson, W.G., Kang, H.K., Eisen, S.A., Murphy, F.M., 2009. Neuropsychological functioning of U.S. Gulf War veterans 10 years after the war. J. Int. Neuropsychol. Soc. : JINS 15, 717–729.

Tynan, R.J., Beynon, S.B., Hinwood, M., Johnson, S.J., Nilsson, M., Woods, J.J., Walker, F.R., 2013. Chronic stress-induced disruption of the astrocyte network is driven by structural atrophy and not loss of astrocytes. Acta Neuropathol. 126, 75–91.

Van Elst, L.T., Maier, S., Fangmeier, T., Endres, D., Mueller, G., Nickel, K., Ebert, D., Lange, T., Hennig, J., Biscaldi, M., 2014. Disturbed cingulate glutamate metabolism in adults with high-functioning autism spectrum disorder: evidence in support of the excitatory/inhibitory imbalance hypothesis. Mol. Psychiatr. 19, 1314–1325.

Vythilingam, M., Luckenbaugh, D.A., Lam, T., Morgan 3rd, C.A., Lipschitz, D., Charney, D.S., Bremner, J.D., Southwick, S.M., 2005. Smaller head of the hippocampus in Gulf War-related posttraumatic stress disorder. Psychiatr. Res. 139, 89–99.

Wallace, M.L., Burette, A.C., Weinberg, R.J., Philpot, B.D., 2012. Maternal loss of Ube3a produces an excitatory/inhibitory imbalance through neuron type-specific synaptic defects. Neuron 74, 793–800.

White, R.F., Steele, L., O'Callaghan, J.P., Sullivan, K., Binns, J.H., Golomb, B.A., Bloom, F.E., Bunker, J.A., Crawford, F., Graves, J.C., Hardie, A., Klimas, N., Knox, M., Meggs, W.J., Melling, J., Philbert, M.A., Grashow, R., 2016. Recent research on Gulf War illness and other health problems in veterans of the 1991 Gulf War: effects of toxicant exposures during deployment. Cortex; J Devoted Study Nervous System Behavior 74, 449–475.

Wohr, M., Orduz, D., Gregory, P., Moreno, H., Khan, U., Vorckel, K.J., Wolfer, D.P., Welzl, H., Gall, D., Schiffmann, S.N., Schwaller, B., 2015. Lack of parvalbumin in mice leads to behavioral deficits relevant to all human autism core symptoms and related neural morphofunctional abnormalities. Transl. Psychiatry 5, e525.

Wolfe, J., Proctor, S.P., Erickson, D.J., Hu, H., 2002. Risk factors for multisymptom illness in US Army veterans of the Gulf War. J Occupational Environ Med 44, 271–281.

Wylie, G., Genova, H., Dobryakova, E., DeLuca, J., Chiaravalloti, N., Falvo, M., Cook, D., 2019. Fatigue in Gulf War Illness is associated with tonically high activation in the executive control network. Neuroimage: Clinic 21, 101641.

Yeh, C.-Y., Vadhwana, B., Verkhratsky, A., Rodríguez, J.J., 2011. Early astrocytic atrophy in the entorhinal cortex of a triple transgenic animal model of Alzheimer's disease. ASN Neuro 3, AN20110025.

Yuen, E.Y., Liu, W., Karatsoreos, I.N., Feng, J., McEwen, B.S., Yan, Z., 2009. Acute stress enhances glutamatergic transmission in prefrontal cortex and facilitates working memory. Proc. Natl. Acad. Sci. U.S.A. 106, 14075–14079.

Yuen, E.Y., Wei, J., Liu, W., Zhong, P., Li, X., Yan, Z., 2012. Repeated stress causes cognitive impairment by suppressing glutamate receptor expression and function in prefrontal cortex. Neuron 73, 962–977.

Zakirova, Z., Crynen, G., Hassan, S., Abdullah, L., Horne, L., Mathura, V., Crawford, F., Ait-Ghezala, G., 2015. A chronic longitudinal characterization of neurobehavioral and neuropathological cognitive impairment in a mouse model of Gulf war agent exposure. Front. Integr. Neurosci. 9, 71.

Zakirova, Z., Reed, J., Crynen, G., Horne, L., Hassan, S., Mathura, V., Mullan, M., Crawford, F., Ait-Ghezala, G., 2017. Complementary proteomic approaches reveal mitochondrial dysfunction, immune and inflammatory dysregulation in a mouse model of Gulf War Illness. *Proteomics*. Clinc Applicat 11.

Zhao, C., Deng, W., Gage, F.H., 2008. Mechanisms and functional implications of adult neurogenesis. Cell 132, 645–660.